Complex magnetic monopoles, geometric phases and quantum evolution in the vicinity of diabolic and exceptional points

2008 J. Phys. A: Math. Theor. 41 485304

(http://iopscience.iop.org/1751-8121/41/48/485304)

IOP PUBLISHING JOURNAL OF PHYSICS A: MATHEMATICAL AND THEORETICAL

J. Phys. A: Math. Theor. **41** (2008) 485304 (25pp) doi:10.1088/1751-8113/41/48/485304

Complex magnetic monopoles, geometric phases and quantum evolution in the vicinity of diabolic and exceptional points

Alexander I Nesterov and F Aceves de la Cruz

Departamento de Física, CUCEI, Universidad de Guadalajara, Guadalajara, Jalisco, Mexico

E-mail: nesterov@cencar.udg.mx and fermincucei@gmail.com

Received 5 May 2008, in final form 30 September 2008
Published 22 October 2008
Online at stacks.iop.org/JPhysA/41/485304

Abstract

We consider the geometric phase and quantum tunneling in the vicinity of diabolic and exceptional points. We show that the geometric phase associated with the degeneracy points is defined by the flux of complex magnetic monopoles. In the limit of weak coupling, the leading contribution to the real part of the geometric phase is given by the flux of the Dirac monopole plus a quadrupole term, and the expansion of the imaginary part starts with a dipole-like field. For a two-level system governed by a generic non-Hermitian Hamiltonian, we derive a formula to compute the non-adiabatic, complex, geometric phase by integrating over the complex Bloch sphere. We apply our results to study a dissipative two-level system driven by a periodic electromagnetic field and show that, in the vicinity of the exceptional point, the complex geometric phase behaves like a step-function. Studying the tunneling process near and at the exceptional point, we find two different regimes: coherent and incoherent. The coherent regime is characterized by Rabi oscillations, with a one-sheeted hyperbolic monopole emerging in this region of the parameters. The two-sheeted hyperbolic monopole is associated with the incoherent regime. We show that the dissipation results in a series of pulses in the complex geometric phase which disappear when the dissipation dies out. Such a strong coupling effect of the environment is beyond the conventional adiabatic treatment of the Berry phase.

PACS numbers: 03.65.Vf, 14.80.Hv, 03.65.−w, 03.67.−a, 11.15.−q

1. Introduction

Recent experimental results providing evidence for the 'magnetic' monopole in the crystal-momentum space [1] and the emergence of 'fictitious magnetic monopoles' in the anomalous

Hall effect of ferromagnetic materials, magnetic superconductors, trapped Λ-type atoms, anisotropic spin systems, noncommutative quantum mechanics, ferromagnetic spinor Bose–Einstein condensates, etc [1–8] have caused a rebirth interest in the Dirac monopole problem. The 'fictitious' monopoles appear in the context of the Berry phase as follows. Assume that, for an adiabatically driven quantum system, the energy levels may cross. Then, in the commonest case of double degeneracy with two linearly independent eigenvectors, the energy surfaces form the sheets of a double cone. The apex of the cones is called a 'diabolic point' [9, 10]. Since, for a generic Hermitian Hamiltonian, the co-dimension of the diabolic point is three, it can be characterized by three parameters: $\mathbf{R} = (X, Y, Z)$. The eigenstates, $|n, \mathbf{R}\rangle$, give rise to the Berry's connection defined by $\mathbf{A}_n(\mathbf{R}) = \mathrm{i}\langle n, \mathbf{R}|\nabla_{\mathbf{R}}|n, \mathbf{R}\rangle$, and the curvature $\mathbf{B}_n = \nabla_{\mathbf{R}} \times \mathbf{A}_n$ associated with $\mathbf{A}_n$ is the field strength of 'magnetic' monopole located at the diabolic point [9, 11]. The Berry phase, $\gamma_n = \oint_{\mathcal{C}} \mathbf{A}_n \cdot \mathrm{d}\mathbf{R}$, is interpreted as a holonomy associated with parallel transport along a circuit $\mathcal{C}$ [12].

Similar treatment of the non-Hermitian Hamiltonian is related to the complex extension of the Berry phase, introduced for the first time by Garrison and Wright [13], and the 'fictitious complex monopole' located at the exceptional point [14]. Note that in contrast to the diabolic point the exceptional point is characterized by a coalescence of eigenvalues and their corresponding eigenvectors. Generally, the exceptional points are associated with non-Hermitian physics and have been observed in various physical systems: laser-induced ionization of atoms, microwave cavities, 'crystals of light', in optics of absorptive media, electronic circuits, etc [15–25].

Since the Garrison and Wright paper was published, the geometric phase for quantum systems governed by non-Hermitian Hamiltonians and complex-valued geometric phase effects in dissipative systems were studied by various authors (for discussions and references see, e.g., [11, 13, 15, 26–38]). However, the behavior of quantum systems in the neighborhood of a degeneracy is still an open problem.

In this paper, we consider the geometric phase and tunneling process near and at the diabolic and exceptional points. We show that for a general non-Hermitian system the geometric phase associated with the degeneracy is described by a *complex magnetic monopole*. We find that the exceptional point is the bifurcation point of the complex geometric phase in parameter space, and the real part of the latter has a jump discontinuity at the exceptional point. We show that the exceptional point is the critical point of the quantum mechanical system, where the topological phase transition occurs in parameter space.

We found two distinct regimes in the tunneling process in the vicinity of the exceptional point: coherent and incoherent. The coherent tunneling is characterized by Rabi oscillations, also known as quantum echoes. We also show that the dissipation results in a series of pulses in the real part of the geometric phase. Such strong coupling with the environment disappears in the absence of dissipation.

The paper is organized as follows. In section 2, general results on the behavior of the eigenvectors at diabolic and exceptional points are presented. In section 3, the complex geometric phase and related 'magnetic' monopoles are discussed. In section 4, a non-adiabatic generalization of the complex Berry phase is introduced and the quantum evolution in the vicinity of the diabolic and exceptional points is studied. In section 5, the results and open problems are discussed.

2. General results on behavior of the eigenvectors at diabolic and exceptional points

It is known that, in parameter space, a set of exceptional points defines a smooth surface of co-dimension 2 for a symmetric/asymmetric complex matrix, co-dimension 1 for a real

asymmetric matrix, and that exceptional points do not exist for a real, symmetric or Hermitian matrix [39]. Let $H(\mathbf{p})$ be a complex $N \times N$ matrix that is smoothly dependent on m and real parameters p_i, where i runs from 1 to m. We assume that the exceptional point occurs for some value of parameters $\mathbf{p} = \mathbf{p}_c$. If $\lambda_k(\mathbf{p})$ are the eigenvalues of $H(\mathbf{p})$, we denote by $|\psi_k(\mathbf{p})\rangle$ and $\langle\tilde{\psi}_k(\mathbf{p})|$ the corresponding right/left eigenvectors:

$$H|\psi_k\rangle = \lambda_k|\psi_k\rangle, \qquad \langle\tilde{\psi}_k|H = \langle\tilde{\psi}_k|\lambda_k. \tag{1}$$

For $\mathbf{p} \neq \mathbf{p}_c$, both systems of left and right eigenvectors form a bi-orthogonal basis [40]

$$\sum_k \frac{|\psi_k\rangle\langle\tilde{\psi}_k|}{\langle\tilde{\psi}_k|\psi_k\rangle} = 1, \qquad \langle\tilde{\psi}_k|\psi_{k'}\rangle = 0, \qquad k \neq k'. \tag{2}$$

At the exceptional point, the eigenvalues, say n and $n+1$, coalesce: $\lambda_n(\mathbf{p}_c) = \lambda_{n+1}(\mathbf{p}_c)$, and the corresponding eigenvectors coincide (up to a complex phase) yielding a single eigenvector $|\psi_{\mathrm{EP}}\rangle$. Now, applying the second set of equations in (2) for $k = n$ and $k = n+1$ we find that, at the degeneracy point, the normalization condition is violated:

$$\langle\tilde{\psi}_{\mathrm{EP}}|\psi_{\mathrm{EP}}\rangle = 0. \tag{3}$$

Since, at the exceptional point, both eigenvalues and eigenvectors merge, forming a Jordan block, it is convenient to introduce an orthonormal basis of this invariant two-dimensional subspace as

$$\langle n|n\rangle = 1, \qquad \langle n+1|n+1\rangle = 1, \qquad \langle n|n+1\rangle = 0, \tag{4}$$

where $|n\rangle \neq |\psi_n\rangle$ and $|n+1\rangle \neq |\psi_{n+1}\rangle$.

Assuming that all other eigenstates are non-degenerate, we find that the set of vectors $\{|\chi_k\rangle, \langle\tilde{\chi}_k|\}$, where $|\chi_n\rangle = |n\rangle$, $\langle\tilde{\chi}_{n+1}| = \langle n+1|$, and

$$|\chi_k\rangle = \frac{|\psi_k\rangle}{\sqrt{\langle\tilde{\psi}_k|\psi_k\rangle}}, \qquad \langle\tilde{\chi}_k| = \frac{\langle\tilde{\psi}_k|}{\sqrt{\langle\tilde{\psi}_k|\psi_k\rangle}}, \qquad \text{for} \quad k \neq n, n+1$$

form a biorthonormal basis. Using this basis, we expand an arbitrary vector ψ as

$$|\psi\rangle = \sum c_k(\mathbf{p})|\chi_k(\mathbf{p})\rangle \tag{5}$$

with the coefficients of expansion defined as $c_k = \langle\tilde{\chi}_k|\psi\rangle$.

From the orthogonality condition, we can see that if $|\psi(\mathbf{p})\rangle \to |\psi_{\mathrm{EP}}\rangle$ while $\mathbf{p} \to \mathbf{p}_c$, all c_k $(k \neq n, n+1)$ vanish at the exceptional point. This implies [31]

$$\lim_{\mathbf{p}\to\mathbf{X_c}} (c_1, \ldots, c_N) = (0, \ldots, c_n(\mathbf{p}_c), c_{n+1}(\mathbf{p}_c), 0, \ldots, 0)\,. \tag{6}$$

Now, let $|\psi\rangle$ be the eigenvector of H,

$$H|\psi(\mathbf{p})\rangle = \lambda(\mathbf{p})|\psi(\mathbf{p})\rangle. \tag{7}$$

Using the expansion (5), we may write

$$|\psi\rangle = \alpha|n\rangle + \beta|n+1\rangle + \sum_{k\neq n,n+1} c_k(\mathbf{p})|\chi_k(\mathbf{p})\rangle. \tag{8}$$

Inserting (8) into equation (7), we find that the coefficients α and β are found from the two-dimensional eigenvalue problem

$$\begin{pmatrix} \lambda_0 + Z & X - \mathrm{i}Y \\ X + \mathrm{i}Y & \lambda_0 - Z \end{pmatrix} \begin{pmatrix} \alpha_\pm \\ \beta_\pm \end{pmatrix} = \lambda_\pm \begin{pmatrix} \alpha_\pm \\ \beta_\pm \end{pmatrix}, \tag{9}$$

where

$$\lambda_0(\mathbf{p}) = \frac{1}{2}(\langle n|H|n\rangle + \langle n+1|H|n+1\rangle), \tag{10}$$

$$X(\mathbf{p}) = \frac{1}{2}(\langle n|H|n+1\rangle + \langle n+1|H|n\rangle), \tag{11}$$

$$Y(\mathbf{p}) = \frac{\mathrm{i}}{2}(\langle n|H|n+1\rangle - \langle n+1|H|n\rangle), \tag{12}$$

$$Z(\mathbf{p}) = \frac{1}{2}(\langle n|H|n\rangle - \langle n+1|H|n+1\rangle). \tag{13}$$

Solving the characteristic equation for (9), we obtain $\lambda_\pm = \lambda_0 \pm \sqrt{X^2+Y^2+Z^2}$. Setting $\mathbf{R}(\mathbf{p}) = (X, Y, Z)$ and $R = \sqrt{X^2+Y^2+Z^2}$, we find that the eigenvalues coalescence at the point $R(\mathbf{p}_c) = 0$. This yields the diabolic point if $X(\mathbf{p}_c) = Y(\mathbf{p}_c) = Z(\mathbf{p}_c) = 0$, and the exceptional point otherwise. Thus, in the vicinity of the level crossing point the N-dimensional problem can be described by the effective two-dimensional non-Hermitian Hamiltonian $H_{\mathrm{ef}}(\mathbf{p}) = \lambda_0(\mathbf{p})\mathbb{1} + \mathbf{R}(\mathbf{p})\cdot\boldsymbol{\sigma}$. However, finding the corresponding two-dimensional space for a general N-dimensional matrix family is a nontrivial problem [39, 41, 42].

3. Degeneracy, geometric phases and complex 'magnetic' monopoles

Following [13], let us consider the time-dependent Schrödinger equation and its adjoint equation:

$$\mathrm{i}\frac{\partial}{\partial t}|\Psi(t)\rangle = H(X(t))|\Psi(t)\rangle, \tag{14}$$

$$-\mathrm{i}\frac{\partial}{\partial t}\langle\widetilde{\Psi}(t)| = \langle\widetilde{\Psi}(t)|H(X(t)), \tag{15}$$

where H is the non-Hermitian Hamiltonian.

Let $\langle\tilde{\psi}_n(X)|$ and $|\psi_n(X)\rangle$ be the left (right) eigenstates corresponding to the eigenvalue E_n. Then, in the adiabatic approximation, the complex geometric phase is given by [13, 26, 27]

$$\gamma_n = \mathrm{i}\oint_C \frac{\langle\tilde{\psi}_n(X)|\mathrm{d}\psi_n(X)\rangle}{\langle\tilde{\psi}_n(X)|\psi_n(X)\rangle} \tag{16}$$

generalizing Berry's result to the dissipative case. Further, we assume that the instantaneous eigenvectors form a bi-orthonormal basis, $\langle\tilde{\psi}_m|\psi_n\rangle = \delta_{mn}$. This can alter the geometric phase (16) up to the topological contribution πn, $n \in \mathbb{Z}$ [43, 44].

For a non-Hermitian Hamiltonian, the validity of the adiabatic approximation is defined by the following condition:

$$\sum_{m\neq n}\left|\frac{\langle\tilde{\psi}_m|\partial H/\partial t|\psi_n(X)\rangle}{(E_m - E_n)^2}\right| \ll 1. \tag{17}$$

This restriction is violated near the degeneracies related to any of the diabolic points or exceptional points, where the eigenvalues coalesce.

Since the adiabatic approach cannot be applied in the neighborhood of a degeneracy, we will consider the non-adiabatic generalization of Berry's phase introduced by Aharonov and Anandan [45] and extended by Garrison and Wright to the non-Hermitian systems as follows

[13]. Let an adjoint pair $\{|\Psi(t)\rangle, \langle\widetilde{\Psi}(t)|\}$ be a solution of equations (14) and (15) satisfying the following condition:

$$|\Psi(T)\rangle = \exp(\mathrm{i}\varphi)|\Psi(0)\rangle, \tag{18}$$

$$\langle\widetilde{\Psi}(T)| = \exp(-\mathrm{i}\varphi)\langle\widetilde{\Psi}(0)|, \tag{19}$$

where φ is complex, and let $\{|\chi(t)\rangle, \langle\tilde{\chi}(t)|\}$ be a modified adjoint pair such that

$$|\chi(t)\rangle = \exp(\mathrm{i}f(t))|\Psi(t)\rangle, \tag{20}$$

$$\langle\tilde{\chi}(t)| = \exp(-\mathrm{i}f(t))\langle\widetilde{\Psi}(t)|, \tag{21}$$

where $f(t)$ is any function satisfying $f(t+T) - f(t) = \varphi(t)$. The total phase φ calculated for the time interval $(0, T)$ may be written as $\varphi = \gamma + \delta$, where the 'dynamical phase' is given by

$$\delta = -\int_0^T \langle\tilde{\chi}(t)|H|\chi(t)\rangle\,\mathrm{d}t, \tag{22}$$

and for the geometric phase γ one has

$$\gamma = \mathrm{i}\int_0^T \langle\tilde{\chi}(t)|\frac{\partial}{\partial t}\chi(t)\rangle\,\mathrm{d}t. \tag{23}$$

This yields the connection 1-form and the curvature 2-form as follows [46]:

$$A = \mathrm{i}\langle\tilde{\chi}|d\chi\rangle, \qquad F = dA. \tag{24}$$

Note that the real part of the geometric phase (23), in addition to the contribution of the usual Berry phase, contains a contribution of environment. Its imaginary part changes the amplitude of the density matrix and implies mixture of the initially pure states.

The geometric phase, γ, for an arbitrary quantum evolution can also be obtained from the total phase, γ_t, by subtracting the dynamical phase, γ_d [36]:

$$\gamma = \gamma_t - \gamma_d, \tag{25}$$

where

$$\gamma_t = \arg\langle\Psi(0)|\Psi(t)\rangle \qquad \text{and} \qquad \gamma_d = -\mathrm{i}\int_0^t \langle\Psi(t)|\frac{\mathrm{d}}{\mathrm{d}t}|\Psi(t)\rangle\,\mathrm{d}t. \tag{26}$$

We adopt and generalize this definition of the geometric phase for non-Hermitian quantum evolution as follows (see also [43]):

$$\gamma = \frac{\mathrm{i}}{2}\ln\frac{\langle\widetilde{\Psi}(t)|\Psi(0)\rangle}{\langle\widetilde{\Psi}(0)|\Psi(t)\rangle} + \mathrm{i}\int_0^t \langle\widetilde{\Psi}(t)|\frac{\mathrm{d}}{\mathrm{d}t}|\Psi(t)\rangle\,\mathrm{d}t. \tag{27}$$

As can be observed, (27) gives a gauge-invariant definition of the geometric phase with respect to gauge transformations:

$$|\Psi\rangle \to \mathrm{e}^{\mathrm{i}\alpha}|\Psi\rangle, \qquad \langle\widetilde{\Psi}| \to \mathrm{e}^{-\mathrm{i}\alpha}\langle\widetilde{\Psi}|, \quad \alpha \in \mathbb{C}. \tag{28}$$

3.1. Two-level system and 'magnetic' monopoles

As has been mentioned before, in the vicinity of the degeneracy point, the behavior of the N-dimensional system can be described by an effective two-dimensional quantum system. In what follows, we consider in detail the complex geometric phase associated with the generic non-Hermitian Hamiltonian:

$$H = \begin{pmatrix} \lambda_0 + Z & X - \mathrm{i}Y \\ X + \mathrm{i}Y & \lambda_0 - Z \end{pmatrix}, \qquad X, Y, Z \in \mathbb{C}, \tag{29}$$

with $X, Y, Z \in \mathbb{C}$ being complex parameters.

For the Hamiltonian (29), the exceptional point is determined by equation

$$X^2 + Y^2 + Z^2 = 0, \tag{30}$$

and defines a hypersurface of complex codimension 1 in $\mathbb{C}^3$, which can also be considered as a smooth surface of codimension 2 in a six-dimensional real space. Note that the diabolic point is just a point in a three-dimensional complex space $\mathbb{C}^3$ and is located at the origin of coordinates.

The solution to the eigenvalue problem

$$H|u\rangle = \lambda|u\rangle, \qquad \langle\tilde{u}|H = \lambda\langle\tilde{u}| \tag{31}$$

where $|u\rangle$ and $\langle\tilde{u}|$ are the right and left eigenvectors, respectively, is given by

$$\lambda_\pm = \lambda_0 \pm R, \tag{32}$$

where $R = (X^2 + Y^2 + Z^2)^{1/2}$. The right and left eigenvectors are found to be

$$|u_+\rangle = \begin{pmatrix} \cos\frac{\theta}{2} \\ \mathrm{e}^{\mathrm{i}\varphi}\sin\frac{\theta}{2} \end{pmatrix}, \qquad \langle\tilde{u}_+| = \left(\cos\frac{\theta}{2}, \mathrm{e}^{-\mathrm{i}\varphi}\sin\frac{\theta}{2}\right) \tag{33}$$

$$|u_-\rangle = \begin{pmatrix} -\mathrm{e}^{-\mathrm{i}\varphi}\sin\frac{\theta}{2} \\ \cos\frac{\theta}{2} \end{pmatrix}, \qquad \langle\tilde{u}_-| = \left(-\mathrm{e}^{\mathrm{i}\varphi}\sin\frac{\theta}{2}, \cos\frac{\theta}{2}\right), \tag{34}$$

where

$$\cos\frac{\theta}{2} = \sqrt{\frac{R+Z}{2R}}, \qquad \sin\frac{\theta}{2} = \sqrt{\frac{R-Z}{2R}}, \tag{35}$$

$$\mathrm{e}^{\mathrm{i}\varphi} = \frac{X+\mathrm{i}Y}{\sqrt{R^2-Z^2}}, \qquad \mathrm{e}^{-\mathrm{i}\varphi} = \frac{X-\mathrm{i}Y}{\sqrt{R^2-Z^2}}, \tag{36}$$

and θ, φ are the complex angles of the complex spherical coordinates:

$$X = R\sin\theta\cos\varphi, \qquad Y = R\sin\theta\sin\varphi, \qquad Z = R\cos\theta. \tag{37}$$

Finally, for $R \neq 0$, the following relationships hold:

$$\langle\tilde{u}_\pm|u_\mp\rangle = 0, \qquad \langle\tilde{u}_\pm|u_\pm\rangle = 1. \tag{38}$$

As seen from equation (32), the coupling of eigenvalues λ_+ and λ_- occurs when $X^2 + Y^2 + Z^2 = 0$. This implies the existence of two cases. The first one, defined by $\theta = 0$, $\varphi = 0$, yields two linearly independent eigenvectors. The point of coupling is known as the diabolic point, and we obtain

$$|u_+\rangle = \begin{pmatrix} 1 \\ 0 \end{pmatrix}, \qquad \langle\tilde{u}_+| = (1,0), \qquad |u_-\rangle = \begin{pmatrix} 0 \\ 1 \end{pmatrix}, \qquad \langle\tilde{u}_-| = (0,1). \tag{39}$$

The second case is characterized by the coupling of eigenvalues and the merging of the eigenvectors. The degeneracy point is known as the exceptional point, and we have $|u_+\rangle = \mathrm{e}^{\mathrm{i}\kappa}|u_-\rangle$ and $\langle\tilde{u}_+| = \mathrm{e}^{-\mathrm{i}\kappa}\langle\tilde{u}_-|$, where $\kappa \in \mathbb{C}$ is a complex phase. Hence, a violation of the normalization condition (38) occurs at the exceptional point, and we have $\langle\tilde{u}_\pm|u_\pm\rangle = 0$.

Let us assume that the exceptional point is given by $\mathbf{R}_0 = (X_0, Y_0, Z_0)$. Then, if $Z_0 \neq 0$, using equations (35)–(37) we obtain

$$\tan\frac{\theta_0}{2} = \pm\mathrm{i}, \qquad \mathrm{e}^{2\mathrm{i}\varphi_0} = \frac{X_0 + \mathrm{i}Y_0}{X_0 - \mathrm{i}Y_0} \tag{40}$$

and, thus, at the exceptional point $\mathrm{Im}\,\theta \to \pm\infty$. If $Z_0 = 0$, we obtain $X_0 = \pm \mathrm{i} Y_0$. This implies $\theta_0 = \pi/2$, and $\mathrm{Im}\,\varphi \to \pm\infty$ at the exceptional point.

Inserting formulae (33)–(34) for $|u_\pm\rangle$ and $\langle\tilde{u}_\pm|$ into (24), we obtain the connection 1-form:

$$A = q(1 - \cos\theta)\,\mathrm{d}\varphi, \tag{41}$$

where $q = \mp 1/2$ and upper/lower sign corresponds to $|u_\pm\rangle$, respectively. The related curvature 2-form reads

$$F = \mathrm{d}A = q \sin\theta \mathrm{d}\theta \wedge \mathrm{d}\varphi, \qquad \theta, \varphi \in \mathbb{C} \tag{42}$$

and, in complex Cartesian coordinates, the connection 1-form and the curvature 2-form can be written as

$$A = \frac{q(X\,\mathrm{d}Y - Y\,\mathrm{d}X)}{R(R+Z)}, \tag{43}$$

$$F = \frac{q}{R^3}\varepsilon_{ijk} X^k\,\mathrm{d}X^i \wedge \mathrm{d}X^j. \tag{44}$$

The obtained formulae describe a complex 'magnetic monopole' with a charge q and the field $B = *F$ given by

$$\mathbf{B} = q\frac{\mathbf{R}}{R^3}, \tag{45}$$

where $\mathbf{R} = (X, Y, Z)$, and $X, Y, Z \in \mathbb{C}$. The field of the monopole can be written as $B^i = -\partial\Phi/\partial X^i$, where the potential $\Phi = q/R$.

The computation of the geometric phase yields

$$\gamma = \oint_{\mathcal{C}} A, \tag{46}$$

where integration is performed over the contour $\mathcal{C}$ on the complex sphere S^2_c. Applying Stokes' theorem, we obtain

$$\gamma = \int_\Sigma F = q\Omega(\mathcal{C}), \tag{47}$$

where Σ is a closed surface with a boundary $\mathcal{C} = \partial\Sigma$, and $\Omega(\mathcal{C})$ is the complex solid angle subtended by the contour $\mathcal{C}$.

Generally, the complex magnetic monopole emerges in quantum mechanical systems with $SL(2, C)$ symmetry. In the particular case of $SO(3)$ symmetry, the related degeneracy is referred to as the diabolic point, and formula (45) reproduces the classical Berry result of a two-fold degeneracy in parameter space [9]. For the exceptional point the field of the corresponding 'monopole' represents a complicated topological charge rather than a point-like magnetic charge. In what follows, we discuss two particular applications: *hyperbolic monopole* and *complex Dirac monopole*.

3.1.1. Hyperbolic monopole. Let us consider the following non-Hermitian Hamiltonian:

$$H = \begin{pmatrix} \lambda_0 + \mathrm{i}z & x - \mathrm{i}y \\ x + \mathrm{i}y & \lambda_0 - \mathrm{i}z \end{pmatrix}, \qquad x, y, z \in \mathbb{R}. \tag{48}$$

The eigenvalues of the Hamiltonian given by $\lambda_\pm = \lambda_0 \pm R$, where $R = (x^2 + y^2 - z^2)^{1/2}$, coalesce at the point $R = 0$. In addition, the exceptional point is represented by a double cone with its apex at the origin, and the diabolic point is also located at the origin.

Applying (43)–(44), we obtain

$$A = \frac{q(x\,\mathrm{d}y - y\,\mathrm{d}x)}{R(R+\mathrm{i}z)} \qquad \text{and} \qquad F = \frac{\mathrm{i}q}{R^3}\varepsilon_{ijk}x^k\,\mathrm{d}x^i \wedge \mathrm{d}x^j. \tag{49}$$

This yields

$$\mathbf{B} = \mathrm{i}q\frac{\mathbf{R}}{R^3}, \qquad \mathbf{R} = (x, y, z). \tag{50}$$

Hence, the field $\mathbf{B}$ can be written as $= -\nabla\Phi$, where $\Phi = -\mathrm{i}q/R$.

For $R^2 > 0$, the surface defined by $R = \text{const}$ is a one-sheeted hyperboloid, which can also be considered as the coset class $SU(1,1)/\mathbb{R} \sim SO(2,1)/SO(1,1)$ [47, 48]. Introducing the inner coordinates (θ, φ) as

$$x = R\cosh\theta\cos\varphi, \qquad y = R\cosh\theta\sin\varphi, \qquad z = R\sinh\theta, \tag{51}$$

where $-\infty \leqslant \theta \leqslant \infty, 0 \leqslant \varphi < 2\pi$, we obtain

$$A = q(1 - \mathrm{i}\sinh\theta)\,\mathrm{d}\varphi, \qquad F = -\mathrm{i}q\cosh\theta\mathrm{d}\theta \wedge \mathrm{d}\varphi. \tag{52}$$

The resultant one-sheeted hyperbolic monopole carries an imaginary total charge $\mathrm{i}q$ and, in contrast to the point-like Dirac monopole, has a singularity on the surface of the double cone identified with the exceptional point.

For $R^2 < 0$, the surface characterized by $z^2 - x^2 - y^2 = \text{const}$ is a two-sheeted hyperboloid. A convenient parametrization is given by

$$x = \tilde{R}\sinh\theta\cos\varphi, \qquad y = \tilde{R}\sinh\theta\sin\varphi, \qquad z = \tilde{R}\cosh\theta \quad (z > 0) \tag{53}$$

$$x = \tilde{R}\sinh\theta\cos\varphi, \qquad y = \tilde{R}\sinh\theta\sin\varphi, \qquad z = -\tilde{R}\cosh\theta \quad (z < 0) \tag{54}$$

where $0 \leqslant \theta \leqslant \infty, 0 \leqslant \varphi < 2\pi, \tilde{R} = (z^2 - x^2 - y^2)^{1/2}$, and we preserve the same notation for the angular coordinates, as above. The relevant coset class is $SU(1,1)/U(1) \sim SO(2,1)/SO(2)$, and referring to (49) and (50), we obtain

$$A^+ = q(1 - \cosh\theta)\,\mathrm{d}\varphi, \qquad F^+ = -q\sinh\theta\mathrm{d}\theta \wedge \mathrm{d}\varphi \quad (z > 0), \tag{55}$$

$$A^- = q(1 + \cosh\theta)\,\mathrm{d}\varphi, \qquad F^- = q\sinh\theta\mathrm{d}\theta \wedge \mathrm{d}\varphi \quad (z < 0). \tag{56}$$

Hence, the monopole carries a real total charge given by $-q$. Note that the two-sheeted hyperbolic monopole has already appeared in the literature in connection with the geometric phase (see, e.g., [47–49]). Moreover, as has been pointed out by Jackiw [48], this is a topologically trivial case, and the curvature may be removed by a globally well-defined canonical transformation.

It can easily be shown that, in the case of a one-sheeted monopole, the corresponding potential Φ is imaginary and, for a two-sheeted hyperbolic monopole, Φ is a real function. In figure 1, the surfaces of $\mathrm{Im}\,\Phi = \text{const}$ and $\mathrm{Re}\,\Phi = \text{const}$ related to the one-sheeted and two-sheeted hyperbolic monopole, respectively, are depicted.

The hyperbolic monopoles appear in a wide class of physical systems with $SO(2,1)$ invariance (for discussion see, e.g., [47–51] and references therein). For instance, the hyperbolic monopole emerges in a two-level atom interacting with an electromagnetic field (see section 4.1.3).

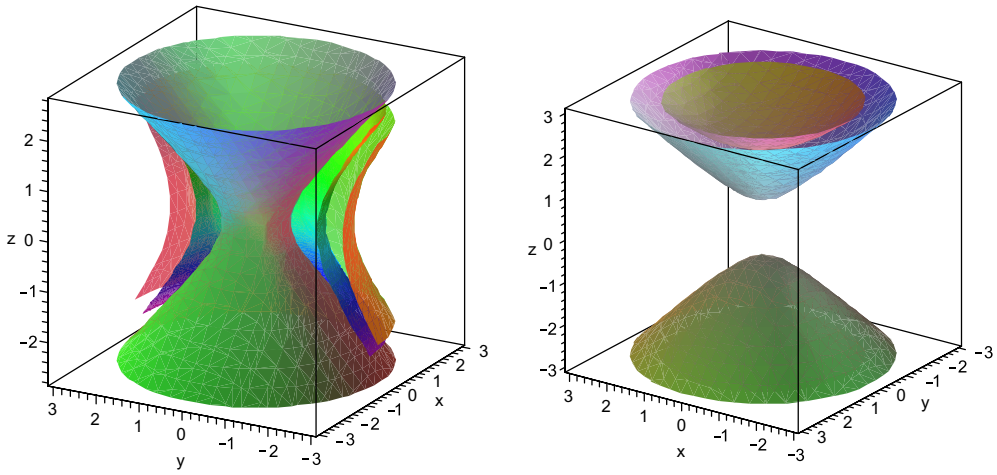

Figure 1. Hyperbolic monopole. Left panel: $R^2 > 0$, one-sheeted hyperbolic monopole. The surfaces $\mathrm{Im}\,\Phi = \mathrm{const}$ are depicted. Right panel: $R^2 < 0$, two-sheeted hyperbolic monopole. The surfaces $\mathrm{Re}\,\Phi = \mathrm{const}$ are presented. The exceptional point is realized as the double-cone (not plotted).

3.1.2. Complex Dirac monopole. Let us consider the non-Hermitian Hamiltonian written as

$$H = \begin{pmatrix} \lambda_0 + z - \mathrm{i}\varepsilon & x - \mathrm{i}y \\ x + \mathrm{i}y & \lambda_0 - z + \mathrm{i}\varepsilon \end{pmatrix}, \qquad x, y, z \in \mathbb{R}. \tag{57}$$

The computation of the 'magnetic' field **B** yields

$$\mathbf{B} = \frac{q\mathbf{R}}{R^3}, \qquad \mathbf{R} = (x, y, z - \mathrm{i}\varepsilon) \tag{58}$$

where $R = (x^2 + y^2 + z^2 - \varepsilon^2 - 2\mathrm{i}\varepsilon z)^{1/2}$. The exceptional point obtained as the solution of equation

$$x^2 + y^2 + z^2 - \varepsilon^2 + 2\mathrm{i}\varepsilon z = 0 \tag{59}$$

is the circle of the radius ε at the plane $z = 0$.

The field of the monopole, $\mathbf{B} = -\nabla\Phi$, is defined by the complex potential $\Phi = q/R$, depicted in figure 2. Setting $r = (x^2 + y^2 + z^2)^{1/2}$ and using the real spherical coordinates (r, α, β), we have $R = (r^2 - 2\mathrm{i}\varepsilon r\cos\alpha - \varepsilon^2)^{1/2}$. Then, we may expand the potential Φ as follows:

$$\Phi = \frac{q}{\sqrt{r^2 - 2\mathrm{i}\varepsilon r\cos\alpha - \varepsilon^2}} = q\sum_{l=0}^{\infty}\frac{(\mathrm{i}\varepsilon)^l}{r^{l+1}}P_l(\cos\alpha). \tag{60}$$

For $r \gg \varepsilon$, this yields

$$\Phi = \frac{q}{r} + \mathrm{i}\frac{p\cos\alpha}{r^2} - \frac{Q(3\cos^2\alpha - 1)}{2r^3} + \cdots, \tag{61}$$

where q is the monopole charge, $p = q\varepsilon$ is the dipole moment, and $Q = q\varepsilon^2$ is the quadrupole moment.

The geometric phase of the ground state is found to be

$$\gamma = q\oint_C\left(1 - \frac{r\cos\alpha - \mathrm{i}\varepsilon}{\sqrt{r^2 - 2\mathrm{i}\varepsilon r\cos\alpha - \varepsilon^2}}\right)\mathrm{d}\beta. \tag{62}$$

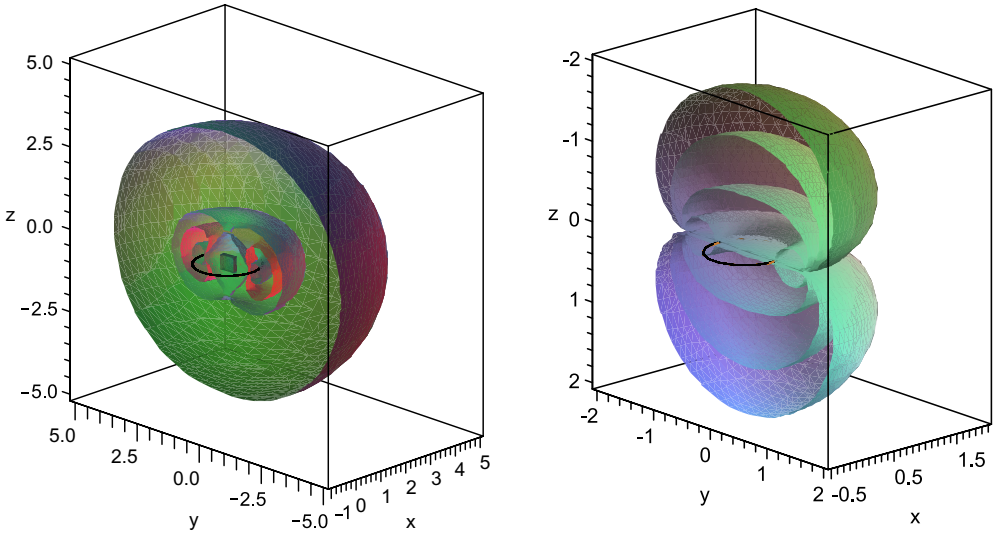

Figure 2. Complex Dirac monopole. The surfaces $\mathrm{Re}\,\Phi = \mathrm{const}$ (left) and $\mathrm{Im}\,\Phi = \mathrm{const}$ (right) are plotted. The exceptional point is depicted by a circle of radius $r = 1 (\varepsilon = 1)$.

Using a multipole expansion (61), we obtain the following expression for γ:

$$\gamma = \gamma_M + \mathrm{i} \oint_{\mathcal{C}} \frac{p \sin^2 \alpha}{r} \, \mathrm{d}\beta - \oint_{\mathcal{C}} \frac{3Q \sin^2 \alpha \cos \alpha}{2r^2} \, \mathrm{d}\beta + \cdots, \tag{63}$$

where $\gamma_M = q \oint_{\mathcal{C}} (1 - \cos \alpha) \, \mathrm{d}\beta$ is the contribution of the Dirac monopole at the origin, the second term describes the dipole contribution to the imaginary part of the geometric phase and the third term is the quadrupole contribution to its real part.

Let us consider the closed curve $\mathcal{C}$ parameterized by β with complex angle $\theta = \mathrm{const}$. Then for $q = 1/2$ the geometric phase (62) becomes

$$\gamma = \pi \left(1 - \frac{z - \mathrm{i}\varepsilon}{\sqrt{\rho^2 + (z - \mathrm{i}\varepsilon)^2}} \right), \tag{64}$$

where $\rho = (x^2 + y^2)^{1/2}$.

A complex Dirac monopole and related complex Berry's phase appear in a wide class of open systems, where the Hamiltonian

$$\tilde{H} = \mathbf{B}(t) \cdot \boldsymbol{\sigma} - \frac{\mathrm{i}}{2} \Gamma^\dagger \Gamma$$

includes spontaneous decay $\Gamma = \sqrt{\varepsilon} \sigma_-$ as a source of decoherence (see, e.g., [37] and references therein). For instance, it emerges in a two-level atom driven by a periodic electromagnetic field $\mathbf{E}(t) = \mathrm{Re}(\boldsymbol{\mathcal{E}}(t) \exp(\mathrm{i}\nu t))$, with $\boldsymbol{\mathcal{E}}(t)$ being slowly varied, as follows. In the rotating wave approximation, after removing the explicit time dependence of the Hamiltonian with a suitable non-unitary transformation, the Schrödinger equation reads [13]

$$\mathrm{i} \begin{pmatrix} \dot{u}_1 \\ \dot{u}_2 \end{pmatrix} = \frac{1}{2} \begin{pmatrix} \Delta - \frac{\mathrm{i}}{2}\gamma_a & 2V^* \\ 2V & -\Delta - \frac{\mathrm{i}}{2}\gamma_b \end{pmatrix} \begin{pmatrix} u_1 \\ u_2 \end{pmatrix}, \tag{65}$$

where γ_a, γ_b are decay rates for the upper and lower levels, respectively, $\Delta = \omega_0 - \nu$, $\omega_0 = (E_a - E_b)$, $V = \boldsymbol{\mu} \cdot \boldsymbol{\mathcal{E}}$ and $\boldsymbol{\mu}$ is the dipole matrix element. To compare the geometric

Table 1. Monopole structure of the two-level dissipative system.

Monopole classification	
Dirac monopole	$\varepsilon = 0$
Complex monopole	$\varepsilon \neq 0$
Complex Dirac monopole	$\varepsilon \neq 0, \varepsilon = \text{const}$
One-sheeted hyperbolic monopole	$\varepsilon \neq 0, z = 0, x^2 + y^2 - \varepsilon^2 > 0$
Two-sheeted hyperbolic monopole	$\varepsilon \neq 0, z = 0, x^2 + y^2 - \varepsilon^2 < 0$

phase (64) with that found in [13], we set $x = \operatorname{Re} V(t)$, $y = \operatorname{Im} V(t)$, $z = \Delta/2$ and $\varepsilon = \delta/2 = (\gamma_a - \gamma_b)/4$. Then, the geometric phase (64) can be written as

$$\gamma = \pi\left(1 - \frac{\Delta - \mathrm{i}\delta}{\sqrt{|2V_0|^2 + (\Delta - \mathrm{i}\delta)^2}}\right) \tag{66}$$

which coincides with the result obtained by Garrison and Wright [13] .

3.1.3. Remark. Comparing (92) with equations (48) and (57), we conclude that both the complex Dirac monopole and the hyperbolic monopole can be realized in the four-dimensional parameter space $x, y, z, \varepsilon \in \mathbb{R}^4$. A brief classification of the monopole structure is given in table 1.

4. Geometric phase and quantum evolution in the vicinity of diabolic and exceptional points

Since the adiabatic approach cannot be applied in the neighborhood of a degeneracy, we here consider a non-adiabatic generalization of the complex Berry phase. Let $|u(t)\rangle$ and $\langle\tilde{u}(t)|$ be solutions of the Schrödinger equation and its adjoint equation:

$$\mathrm{i}\frac{\partial}{\partial t}|u(t)\rangle = H|u(t)\rangle, \tag{67}$$

$$-\mathrm{i}\frac{\partial}{\partial t}\langle\tilde{u}(t)| = \langle\widetilde{u}(t)|H, \tag{68}$$

where we assume, as usual, the normalization condition $\langle\tilde{u}(t)|u(t)\rangle = 1$. For an arbitrary evolution of a non-Hermitian quantum system, the complex geometric phase $\gamma = \gamma_t - \gamma_d$ is given by equation (27), and we have

$$\gamma = \frac{\mathrm{i}}{2}\ln\frac{\langle\tilde{u}(t)|u(0)\rangle}{\langle\tilde{u}(0)|u(t)\rangle} + \mathrm{i}\int_0^t \langle\tilde{u}(t)|\dot{u}(t)\rangle\,\mathrm{d}t. \tag{69}$$

This result can be adopted to calculate the geometric phase over the complex Bloch sphere as follows. Let $\mathbf{n}(t) = (\sin\alpha\cos\beta, \sin\alpha\sin\beta, \cos\alpha)$ be a unit complex Bloch vector defined as $\mathbf{n}(t) = \langle\tilde{u}(t)|\boldsymbol{\sigma}|u(t)\rangle$. The Bloch vector satisfies the following equation:

$$\mathrm{d}\mathbf{n}/\mathrm{d}t = \boldsymbol{\Omega}\times\mathbf{n}, \qquad \boldsymbol{\Omega}(t) = \operatorname{Tr}(H(t)\boldsymbol{\sigma}) \tag{70}$$

and, as shown in the appendix, the complex geometric phase can be written as

$$\gamma = -\frac{1}{2}\int_0^\tau (1 - \cos\alpha)\dot{\beta}\,\mathrm{d}t + \arctan\frac{\sin(\beta_f - \beta_i)}{\cot(\alpha_f/2)\cot(\alpha_i/2) + \cos(\beta_f - \beta_i)}. \tag{71}$$

The integration is performed along the unique curve $\mathbf{n}(t)$ on the unit sphere S_c^2, joining the initial point $\mathbf{n}(0) = \mathbf{n}_i = (\sin\alpha_i \cos\beta_i, \sin\alpha_i \sin\beta_i, \cos\alpha_i)$ and the final point $\mathbf{n}(\tau) = \mathbf{n}_f = (\sin\alpha_f \cos\beta_f, \sin\alpha_f \sin\beta_f, \cos\alpha_f)$.

Under a cyclic quantum evolution with period T, the Bloch vector describes a closed curve $\mathcal{C}$ on the complex two-dimensional sphere S_c^2, and $\mathbf{n}(t+T) = \mathbf{n}(t)$. The associated complex geometric phase, being half of the complex solid angle enclosed by $\mathcal{C}$,

$$\gamma = -\frac{1}{2}\oint (1 - \cos\alpha)\, \mathrm{d}\beta = -\frac{1}{2}\Omega(\mathcal{C}), \tag{72}$$

is known as the complex Aharonov–Anandan phase [13, 52].

Consider a generic non-Hermitian Hamiltonian

$$H = \frac{\lambda_0}{2}\mathbb{1} + \frac{1}{2}\boldsymbol{\Omega}\cdot\boldsymbol{\sigma}, \tag{73}$$

where $\mathbb{1}$ denotes the identity operator. Let $|u_i\rangle$ be a given initial state, then the solution of the Schrödinger equation (71) can be written as $|u(t)\rangle = U(t)|u_i\rangle$ and $\langle\tilde{u}(t) = \langle\tilde{u}_i|U^{-1}(t)$, where

$$U(t) = \left(\cos\frac{\Omega t}{2} - \mathrm{i}\sin\frac{\Omega t}{2}\hat{\boldsymbol{\Omega}}\cdot\boldsymbol{\sigma}\right)\mathrm{e}^{-\mathrm{i}\lambda_0 t/2} \tag{74}$$

$$U^{-1}(t) = \left(\cos\frac{\Omega t}{2} + \mathrm{i}\sin\frac{\Omega t}{2}\hat{\boldsymbol{\Omega}}\cdot\boldsymbol{\sigma}\right)\mathrm{e}^{\mathrm{i}\lambda_0 t/2}, \tag{75}$$

with $\hat{\boldsymbol{\Omega}}$ being the complex unit vector and $\Omega = (\boldsymbol{\Omega}\cdot\boldsymbol{\Omega})^{1/2}$.

Let $|u_i\rangle$ and $|u_f\rangle = |u(t)\rangle$ be the initial and final states, respectively. Denoting the associated adjoint states by $\langle\tilde{u}_i|$ and $\langle\tilde{u}_f|$, we compute the transition amplitude $|u_i\rangle \to |u_i\rangle$ and $|u_i\rangle \to |u_f\rangle$ as

$$T_{ii} = \langle\tilde{u}_i|U(t)|u_i\rangle = \left(\cos\frac{\Omega t}{2} - \mathrm{i}\sin\frac{\Omega t}{2}\mathbf{n}_i\cdot\hat{\boldsymbol{\Omega}}\right)\mathrm{e}^{-\mathrm{i}\lambda_0 t/2} \tag{76}$$

$$T_{fi} = \langle\tilde{u}_f|U(t)|u_i\rangle = \left(\cos\theta_{fi}\cos\frac{\Omega t}{2} - \mathrm{i}\sin\frac{\Omega t}{2}\mathbf{n}_{fi}\cdot\hat{\boldsymbol{\Omega}}\right)\mathrm{e}^{-\mathrm{i}\lambda_0 t/2}, \tag{77}$$

where $\cos\theta_{fi} = \langle\tilde{u}_f|u_i\rangle$, $\mathbf{n}_i = \langle\tilde{u}_i|\boldsymbol{\sigma}|u_i\rangle$ and $\mathbf{n}_{fi} = \langle\tilde{u}_f|\boldsymbol{\sigma}|u_i\rangle$.

The computation of the time-dependent Bloch vector results in

$$\mathbf{n}(t) = \cos\Omega t\mathbf{n}_i + \cos\chi(1 - \cos\Omega t)\hat{\boldsymbol{\Omega}} + \sin\Omega t(\hat{\boldsymbol{\Omega}}\times\mathbf{n}_i), \tag{78}$$

where χ is the angle between the vectors $\mathbf{n}_i$ and $\hat{\boldsymbol{\Omega}}$ such that $\cos\chi = \mathbf{n}_i\cdot\hat{\boldsymbol{\Omega}}$.

Of special interest is the case where $\mathrm{Im}(\boldsymbol{\Omega}\cdot\boldsymbol{\Omega}) = 0$. From $\Omega_0 = (|\boldsymbol{\Omega}\cdot\boldsymbol{\Omega}|)^{1/2}$, we obtain

$$\mathbf{n}(t) = \cos\Omega_0 t\mathbf{n}_i + \cos\chi_0(1 - \cos\Omega_0 t)\frac{\boldsymbol{\Omega}}{\Omega_0} + \frac{\sin\Omega_0 t}{\Omega_0}(\hat{\boldsymbol{\Omega}}\times\mathbf{n}_i), \qquad \text{if} \quad \boldsymbol{\Omega}\cdot\boldsymbol{\Omega} > 0 \tag{79}$$

$$\mathbf{n}(t) = \cosh\Omega_0 t\mathbf{n}_i - \cos\chi_0(1 - \cosh\Omega_0 t)\frac{\boldsymbol{\Omega}}{\Omega_0} + \frac{\sinh\Omega_0 t}{\Omega_0}(\hat{\boldsymbol{\Omega}}\times\mathbf{n}_i), \qquad \text{if} \quad \boldsymbol{\Omega}\cdot\boldsymbol{\Omega} < 0 \tag{80}$$

where $\cos\chi_0 = \mathbf{n}_i\cdot\boldsymbol{\Omega}/\Omega_0$. At the exceptional point given by $\Omega = 0$ and $\boldsymbol{\Omega} = \boldsymbol{\Omega}_e$, both regimes yield

$$\mathbf{n}(t) = \mathbf{n}_i - t(\mathbf{n}_i\times\boldsymbol{\Omega}_e) + \frac{t^2}{2}(\mathbf{n}_i\cdot\boldsymbol{\Omega}_e)\boldsymbol{\Omega}_e. \tag{81}$$

A similar consideration of the transition amplitude yields

$$\left.\begin{aligned} T_{ii} &= \left(\cos\frac{\Omega t}{2} - \mathrm{i}\sin\frac{\Omega t}{2}\mathbf{n}_i\cdot\frac{\boldsymbol{\Omega}}{\Omega_0}\right)\mathrm{e}^{-\mathrm{i}\lambda_0 t/2} \\ T_{fi} &= \left(\cos\theta_{fi}\cos\frac{\Omega t}{2} - \mathrm{i}\sin\frac{\Omega t}{2}\mathbf{n}_{fi}\cdot\frac{\boldsymbol{\Omega}}{\Omega_0}\right)\mathrm{e}^{-\mathrm{i}\lambda_0 t/2} \end{aligned}\right\} \quad \text{if} \quad \boldsymbol{\Omega}\cdot\boldsymbol{\Omega} > 0 \tag{82}$$

and

$$\left.\begin{aligned} T_{ii} &= \left(\cosh\frac{\Omega t}{2} - \mathrm{i}\sinh\frac{\Omega t}{2}\mathbf{n}_i\cdot\frac{\boldsymbol{\Omega}}{\Omega_0}\right)\mathrm{e}^{-\mathrm{i}\lambda_0 t/2} \\ T_{fi} &= \left(\cos\theta_{fi}\cosh\frac{\Omega t}{2} - \mathrm{i}\sinh\frac{\Omega t}{2}\mathbf{n}_{fi}\cdot\frac{\boldsymbol{\Omega}}{\Omega_0}\right)\mathrm{e}^{-\mathrm{i}\lambda_0 t/2} \end{aligned}\right\} \quad \text{if} \quad \boldsymbol{\Omega}\cdot\boldsymbol{\Omega} < 0. \tag{83}$$

Thus, if $\boldsymbol{\Omega}\cdot\boldsymbol{\Omega} > 0$ we obtain *coherent* evolution of the quantum-mechanical system, and if $\boldsymbol{\Omega}\cdot\boldsymbol{\Omega} < 0$ we have an *incoherent* one. At the exceptional point both regimes yield

$$T_{ii} = \left(1 - \mathrm{i}\frac{t}{2}\mathbf{n}_i\cdot\boldsymbol{\Omega}_e\right)\mathrm{e}^{-\mathrm{i}\lambda_0 t/2} \tag{84}$$

$$T_{fi} = \left(\cos\theta_{fi} - \mathrm{i}\frac{t}{2}\mathbf{n}_{fi}\cdot\boldsymbol{\Omega}_e\right)\mathrm{e}^{-\mathrm{i}\lambda_0 t/2}. \tag{85}$$

The complex geometric phase can be derived from formula (69) or equivalently, using (71). Employing (69), we obtain the time-dependent geometric phase

$$\gamma(t) = \frac{\Omega t}{2}\cos\chi + \frac{\mathrm{i}}{2}\ln\frac{1 + \mathrm{i}\cos\chi\tan\frac{\Omega t}{2}}{1 - \mathrm{i}\cos\chi\tan\frac{\Omega t}{2}}. \tag{86}$$

In the vicinity of the exceptional point, we have

$$\gamma(t) = \mathbf{n}_i\cdot\boldsymbol{\Omega}_e\frac{t}{2} + \frac{\mathrm{i}}{2}\ln\frac{1 + \mathrm{i}\mathbf{n}_i\cdot\boldsymbol{\Omega}_e\frac{t}{2}}{1 - \mathrm{i}\mathbf{n}_i\cdot\boldsymbol{\Omega}_e\frac{t}{2}} + \mathcal{O}(\Omega^2). \tag{87}$$

It follows from here that the real part of the geometric phase $\mathrm{Re}\,\gamma(t)$ behaves like a step-function at the point $t_0 = 2/|\mathrm{Im}(\mathbf{n}_i\cdot\boldsymbol{\Omega}_e)|$ (see figures 3 and 4). In particular, we obtain

$$\mathrm{Re}\,\gamma(t_0) = \lim_{\mathrm{Re}(\mathbf{n}_i\cdot\boldsymbol{\Omega}_e)\to 0}\lim_{t\to t_0}\mathrm{Re}\,\gamma(t) = \begin{cases} 0, & \mathrm{Re}(\mathbf{n}_i\cdot\boldsymbol{\Omega}_e)\to 0, & t\to t_0 - 0 \\ -\pi/2, & \mathrm{Re}(\mathbf{n}_i\cdot\boldsymbol{\Omega}_e)\to +0, & t\to t_0 + 0 \\ \pi/2, & \mathrm{Re}(\mathbf{n}_i\cdot\boldsymbol{\Omega}_e)\to -0, & t\to t_0 + 0. \end{cases} \tag{88}$$

4.1. Two-level atom driven by a periodic electromagnetic field

As an illustrative example we consider a two-level dissipative system driven by a periodic electromagnetic field $\mathbf{E}(t) = \mathrm{Re}(\boldsymbol{\mathcal{E}}(t)\exp(\mathrm{i}\nu t))$. In the rotating wave approximation, after removing the explicit time dependence of the Hamiltonian and the average effect of the decay terms, the Schrödinger equation reads [13, 53]

$$\mathrm{i}\begin{pmatrix}\dot{u}_1\\ \dot{u}_2\end{pmatrix} = \frac{1}{2}\begin{pmatrix}-\mathrm{i}\lambda + \Delta - \mathrm{i}\delta & 2V^* \\ 2V & -\mathrm{i}\lambda - \Delta + \mathrm{i}\delta\end{pmatrix}\begin{pmatrix}u_1\\ u_2\end{pmatrix}, \tag{89}$$

where $\lambda = (\gamma_a + \gamma_b)/2$ with γ_a, γ_b being decay rates for upper and lower levels, respectively, $\Delta = \omega_0 - \nu$, $\omega_0 = (E_a - E_b)$, $\delta = (\gamma_a - \gamma_b)/2$, $V = \boldsymbol{\mu}\cdot\boldsymbol{\mathcal{E}}$ and $\boldsymbol{\mu}$ is the dipole matrix element.

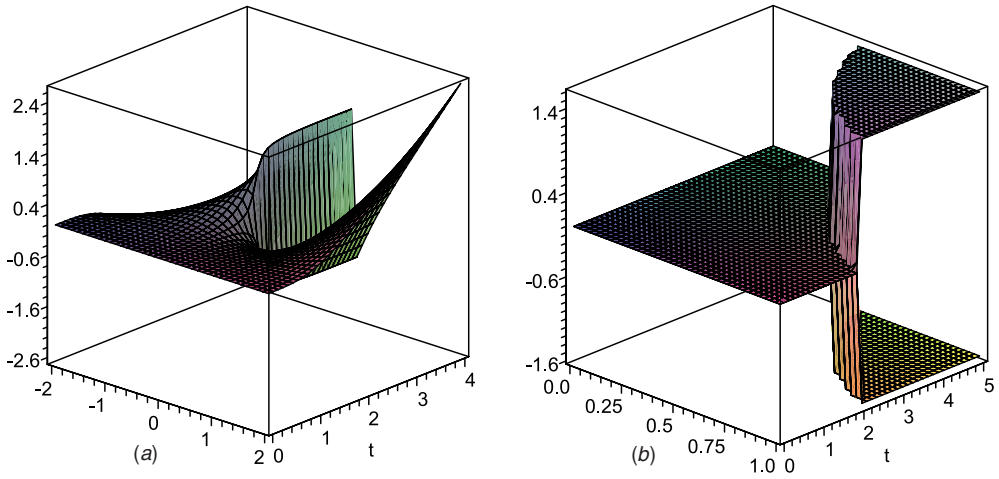

Figure 3. Left panel: the real part of the geometric phase $\mathrm{Re}\,\gamma$ versus $a = \mathrm{Re}(\mathbf{n}_i \cdot \Omega_e)$ and t $(\mathrm{Re}(\mathbf{n}_i \cdot \Omega_e) = 1)$. Right panel: $\mathrm{Re}\,\gamma$ versus $b = \mathrm{Im}(\mathbf{n}_i \cdot \Omega_e)$ and t $(\mathrm{Re}(\mathbf{n}_i \cdot \Omega_e) = 0)$.

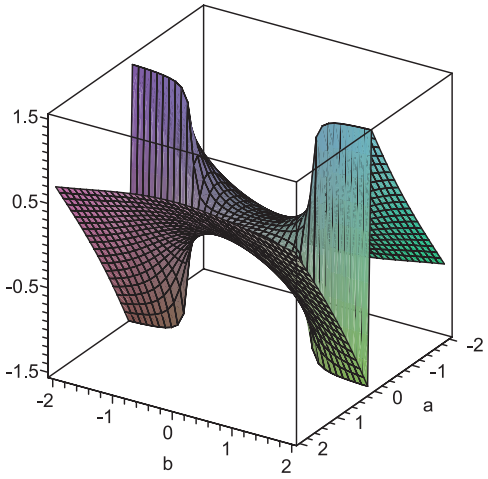

Figure 4. The graphic of $\mathrm{Re}\,\gamma$ as function of $a = \mathrm{Re}(\mathbf{n}_i \cdot \Omega_e)$ and $b = \mathrm{Im}(\mathbf{n}_i \cdot \Omega_e)$ $(t = 2)$.

The choice $\boldsymbol{\mathcal{E}}(t) = \boldsymbol{\mathcal{E}}_0 \exp(\mathrm{i}\omega t)$ yields $V(t) = V_0 \exp(\mathrm{i}\omega t)$, where $V_0 = \boldsymbol{\mu} \cdot \boldsymbol{\mathcal{E}}_0$, and we further assume that $V_0 > 0$. The solution of equation (89) with this choice of $\boldsymbol{\mathcal{E}}$ is well known and can be written as

$$|u(t)\rangle = C_1(t)\,\mathrm{e}^{-\mathrm{i}(\omega - \mathrm{i}\lambda)t/2}|u_\uparrow\rangle + C_2(t)\,\mathrm{e}^{\mathrm{i}(\omega + \mathrm{i}\lambda)t/2}|u_\downarrow\rangle, \tag{90}$$

where $|u_\uparrow\rangle = \binom{1}{0}$ and $|u_\downarrow\rangle = \binom{0}{1}$ denote the up/down states, respectively. In addition, $|C(t)\rangle$ satisfies the Schrödinger equation

$$\mathrm{i}\frac{\partial |C\rangle}{\partial t} = H_r|C\rangle \tag{91}$$

written in a co-rotating reference frame, where the Hamiltonian of the system takes the form

$$H_r = \frac{1}{2}\begin{pmatrix} \Delta - \omega - \mathrm{i}\delta & 2V_0 \\ 2V_0 & -\Delta + \omega + \mathrm{i}\delta \end{pmatrix} \tag{92}$$

and we find

$$\begin{pmatrix} C_1(t) \\ C_2(t) \end{pmatrix} = \begin{pmatrix} \cos(\Omega t/2) - \mathrm{i}\cos\chi\,\sin(\Omega t/2) & -\mathrm{i}\sin\chi\,\sin(\Omega t/2) \\ -\mathrm{i}\sin\chi\,\sin(\Omega t/2) & \cos(\Omega t/2) + \mathrm{i}\cos\chi\,\sin(\Omega t/2) \end{pmatrix} \begin{pmatrix} C_1(0) \\ C_2(0) \end{pmatrix}, \tag{93}$$

where $\cos\chi = (\Delta - \omega - \mathrm{i}\delta)/\Omega$, $\Omega = (\rho^2 + (\Delta - \omega - \mathrm{i}\delta)^2)^{1/2}$, $\rho = 2V_0$.

Passing on to the Bloch vector $\mathbf{n}(t) = \langle\tilde{u}(t)|\boldsymbol{\sigma}|u(t)\rangle$ we obtain

$$\mathbf{n}(t) = \begin{pmatrix} \cos\omega t & -\sin\omega t & 0 \\ \sin\omega t & \cos\omega t & 0 \\ 0 & 0 & 1 \end{pmatrix} \times \begin{pmatrix} \sin^2\chi + \cos^2\chi\,\cos\Omega t & -\cos\chi\,\sin\Omega t & \frac{1}{2}\sin 2\chi(1-\cos\Omega t) \\ \cos\chi\,\sin\Omega t & \cos\Omega t & -\sin\chi\,\sin\Omega t \\ \frac{1}{2}\sin 2\chi(1-\cos\Omega t) & \sin\chi\,\sin\Omega t & \cos^2\chi + \sin^2\chi\,\cos\Omega t \end{pmatrix} \mathbf{n}(0)\,. \tag{94}$$

Finally, one can show that $\mathbf{n}(t)$ satisfies the following equation:

$$\mathrm{d}\mathbf{n}/\mathrm{d}t = \boldsymbol{\Omega}'(t) \times \mathbf{n} \tag{95}$$

where $\boldsymbol{\Omega}' = (\rho\cos\omega t, \rho\sin\omega t, \Delta - \mathrm{i}\delta)$.

4.1.1. Cyclic evolution. Let $\mathbf{n}(t+T) = \mathbf{n}(t)$ be the Bloch vector yielding a cyclic evolution of the system over the complex sphere S_c^2 with a period $T = 2\pi/\omega$. Starting with the definition $\mathbf{n} = \langle\tilde{u}(t)|\boldsymbol{\sigma}|u(t)\rangle$, where $|u(t)\rangle$ and $\langle\tilde{u}(t)|$ satisfy the Schrödinger equation (89) and its adjoint equation, respectively, we find that the solution

$$|u_+(t)\rangle = \cos\frac{\chi}{2}\,\mathrm{e}^{-\mathrm{i}(\omega+\Omega-\mathrm{i}\lambda)t/2}|u_\uparrow\rangle + \sin\frac{\chi}{2}\,\mathrm{e}^{\mathrm{i}(\omega-\Omega+\mathrm{i}\lambda)t/2}|u_\downarrow\rangle \tag{96}$$

$$\langle\tilde{u}_+(t)| = \cos\frac{\chi}{2}\,\mathrm{e}^{\mathrm{i}(\omega+\Omega-\mathrm{i}\lambda)t/2}\langle u_\uparrow| + \sin\frac{\chi}{2}\,\mathrm{e}^{-\mathrm{i}(\omega-\Omega+\mathrm{i}\lambda)t/2}\langle u_\downarrow| \tag{97}$$

yields

$$\mathbf{n}_+ = (\sin\chi\,\cos\omega t, \sin\chi\,\sin\omega t, \cos\chi). \tag{98}$$

Note that $\mathbf{n}_+(t)$ can be obtained as the periodic solution of the Bloch equation with $\boldsymbol{\Omega} = \Omega(\sin\chi, 0, \cos\chi)$. The other periodic solution is given by

$$\mathbf{n}_- = -(\sin\chi\,\cos\omega t, \sin\chi\,\sin\omega t, \cos\chi) \tag{99}$$

and the related solution of the Schrödinger equation reads

$$|u_-(t)\rangle = -\sin\frac{\chi}{2}\,\mathrm{e}^{-\mathrm{i}(\omega+\Omega-\mathrm{i}\lambda)t/2}|u_\uparrow\rangle + \cos\frac{\chi}{2}\,\mathrm{e}^{\mathrm{i}(\omega-\Omega+\mathrm{i}\lambda)t/2}|u_\downarrow\rangle \tag{100}$$

$$\langle\tilde{u}_-(t)| = -\sin\frac{\chi}{2}\,\mathrm{e}^{\mathrm{i}(\omega+\Omega-\mathrm{i}\lambda)t/2}\langle u_\uparrow| + \cos\frac{\chi}{2}\,\mathrm{e}^{-\mathrm{i}(\omega-\Omega+\mathrm{i}\lambda)t/2}\langle u_\downarrow|. \tag{101}$$

The geometric phase derived from (72) is given by

$$\gamma_\pm = -\pi\left(1 \mp \frac{\Delta - \omega - \mathrm{i}\delta}{\sqrt{\rho^2 + (\Delta - \omega - \mathrm{i}\delta)^2}}\right). \tag{102}$$

In the adiabatic limit, $|\omega/(\Delta - \mathrm{i}\delta)| \ll 1$, the complex Aharonov–Anandan phase $\gamma = \gamma_- + 2\pi$ reduces to the complex Berry phase γ_{ad} obtained in [13]:

$$\gamma_{ad} = \pi\left(1 - \frac{\Delta - \mathrm{i}\delta}{\sqrt{(2V_0)^2 + (\Delta - \mathrm{i}\delta)^2}}\right). \tag{103}$$

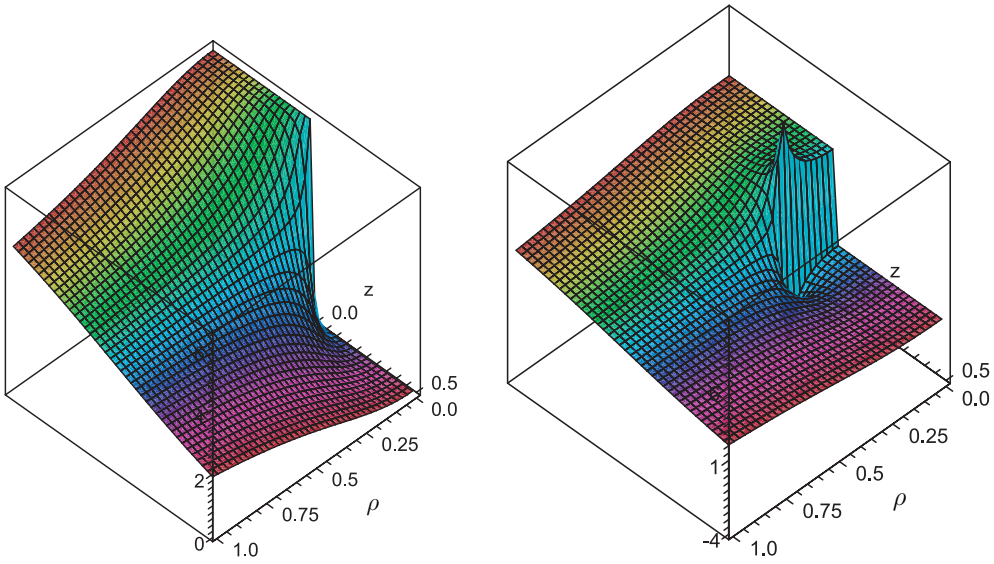

Figure 5. Left panel: the real part of the geometric phase, $\mathrm{Re}\,\gamma$ versus ρ and $z = \Delta - \omega$, in the vicinity of the diabolic point given by $\rho = z = 0$ ($\delta = 0$). Right panel: $\mathrm{Re}\,\gamma$ versus ρ and z nearby the exceptional point defined by $\rho = \delta$ and $z = 0$ ($\delta = 0.25$).

In what follows, we consider the behavior of the geometric phase γ near the critical points, starting with the diabolic point. In this case, $\mathrm{Im}\,\gamma = 0$ and we have

$$\gamma = \pi\left(1 - \frac{\Delta - \omega}{\sqrt{\rho^2 + (\Delta - \omega)^2}}\right). \tag{104}$$

This yields

$$\gamma = \begin{cases} 0, & \text{for} \quad \rho = 0, \quad \Delta - \omega > 0 \\ 2\pi, & \text{for} \quad \rho = 0, \quad \Delta - \omega < 0 \end{cases} \tag{105}$$

It follows that the geometric phase behaves like a step-function near the diabolic point, and that at the diabolic point γ has a jump discontinuity with a gap of 2π (figure 5).

Referring to (102), we find that near the exceptional point, and for $\Delta = \omega$, the real part of the geometric phase is given by

$$\mathrm{Re}\,\gamma = \begin{cases} \pi, & \text{if} \quad \rho > \delta \\ \pi\left(1 \pm \dfrac{\delta}{\sqrt{\delta^2 - \rho^2}}\right), & \text{if} \quad \rho < \delta, \end{cases} \tag{106}$$

where the upper/lower sign corresponds to $\Delta - \omega \to \pm 0$. A similar consideration of the imaginary part of the geometric phase yields

$$\mathrm{Im}\,\gamma = \begin{cases} 0, & \text{if} \quad \rho < \delta \\ \dfrac{\pi\delta}{\sqrt{\rho^2 - \delta^2}}, & \text{if} \quad \rho > \delta. \end{cases} \tag{107}$$

In figure 5, one can see that the geometric phase has an infinite gap at the exceptional point. This is due to the coalescence of eigenvectors at the exceptional point.

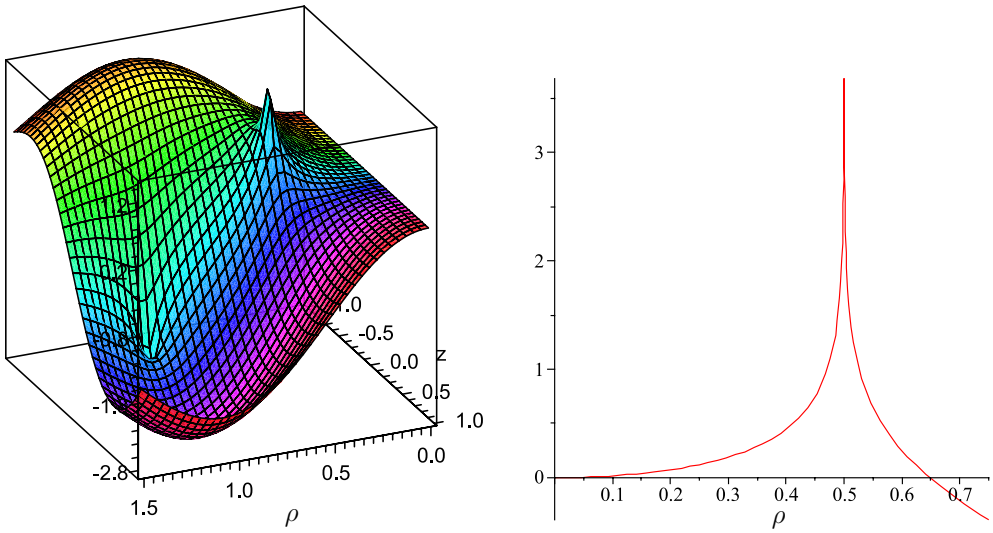

Figure 6. Left panel: the imaginary part of the geometric phase, $\mathrm{Im}\,\gamma$ as function of ρ and $z = \Delta - \omega$ ($t = 2/\delta, \delta = 0.5, \omega = 1$). Right panel: $\mathrm{Im}\,\gamma$ versus ρ ($z = 0, t = 2/\delta, \delta = 0.5, \omega = 1$). The divergence of $\mathrm{Im}\,\gamma$ can be observed at the exceptional point ($\rho = \delta = 0.5, z = 0$).

4.1.2. Non-cyclic evolution. Let us consider the case in which the initial state is $|u(0)\rangle = |u_\uparrow\rangle$, which corresponds to the north pole of the Bloch sphere S_c^2, and, hence, $\mathbf{n}(0) = (0, 0, 1)$. For non-cyclic evolution and an initial state chosen as $\mathbf{n}_i = (0, 0, 1)$, the explicit form of the time-dependent solution of equation (70) is given by

$$\mathbf{n}(t) = \begin{pmatrix} \sin\chi\cos\chi(1-\cos\Omega t)\cos\omega t + \sin\chi\sin\Omega t\sin\omega t \\ \sin\chi\cos\chi(1-\cos\Omega t)\sin\omega t - \sin\chi\sin\Omega t\cos\omega t \\ \cos^2\chi + \sin^2\chi\cos\Omega t \end{pmatrix}. \tag{108}$$

The geometric phase derived from (71) is given by

$$\gamma = \frac{\Omega t}{2}\cos\chi - \frac{\omega\sin^2\chi}{2\Omega}(\Omega t - \sin\Omega t) + \frac{\mathrm{i}}{2}\ln\frac{1+\mathrm{i}\cos\chi\tan\frac{\Omega t}{2}}{1-\mathrm{i}\cos\chi\tan\frac{\Omega t}{2}}, \tag{109}$$

where $\Omega = (\rho^2 + (\Delta - \omega - \mathrm{i}\delta)^2)^{1/2}$. As depicted in figures 6 and 7, the geometric phase has a singular behavior in the vicinity of the exceptional point. At the exceptional point, the imaginary part of the geometric phase diverges, and its real part behaves like a step-function.

In the vicinity of the degeneracy point defined by $\Omega = 0$,

$$\gamma = \frac{Zt}{2} - \frac{\omega\rho^2 t^3}{6} + \frac{\mathrm{i}}{2}\ln\frac{1+\mathrm{i}\frac{Zt}{2}\left(1+\frac{1}{3}\left(\frac{\Omega t}{2}\right)^2\right)}{1-\mathrm{i}\frac{Zt}{2}\left(1+\frac{1}{3}\left(\frac{\Omega t}{2}\right)^2\right)} + \mathcal{O}(\Omega^4), \tag{110}$$

where $Z = \Delta - \omega - \mathrm{i}\delta$. If $t \neq 2/\delta$, it follows that, at the exceptional point defined by $Z = -\mathrm{i}\delta$ and $\rho = \delta$, the geometric phase is given by

$$\gamma = -\frac{\omega\delta^2 t^3}{6} - \mathrm{i}\frac{\delta t}{2} + \frac{\mathrm{i}}{2}\ln\frac{1+\frac{\delta t}{2}}{1-\frac{\delta t}{2}}. \tag{111}$$

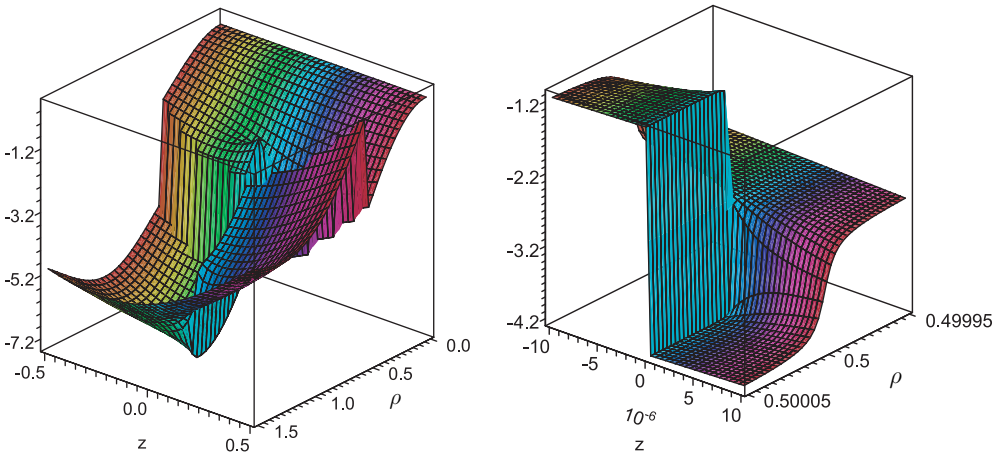

Figure 7. Left panel: the real part of the geometric phase, $\mathrm{Re}\,\gamma$, versus ρ and $z = \Delta - \omega$ ($t = 2/\delta = 0.5, \delta = 0.5, \omega = 1$). Right panel: the same graphic nearby the exceptional point defined by $\rho = \delta$ and $z = 0$.

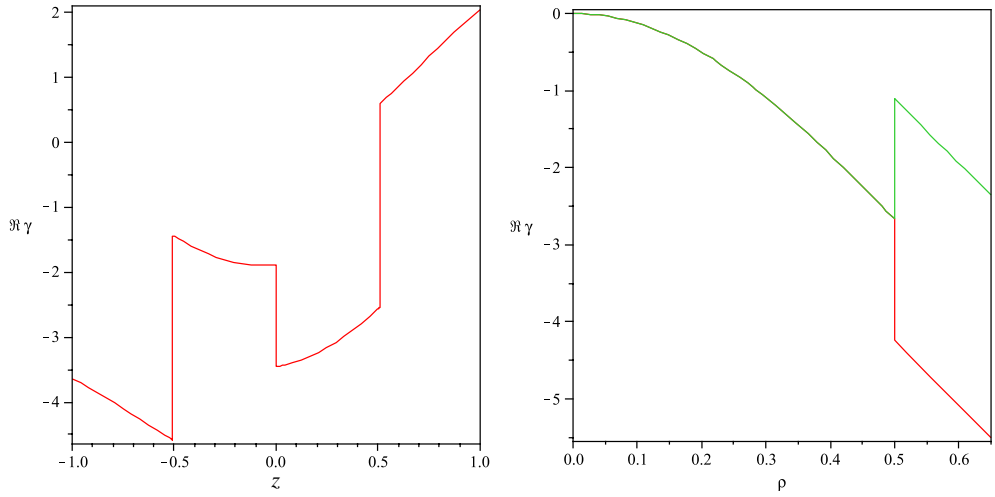

Figure 8. Left panel: graphic of $\mathrm{Re}\,\gamma$ versus $z = \Delta - \omega$ depicted for $t = 2/\delta$ and $\rho = \delta$ ($\delta = 0.5, \omega = 1$). At the exceptional point, defined by $\rho = \delta$ and $z = 0$, the jump discontinuity is given by $\Delta\mathrm{Re}\,\gamma = \pm\pi/4$. Right panel: $\mathrm{Re}\,\gamma$ versus ρ ($t = 2/\delta, z = 0, \delta = 0.5, \omega = 1$). At the exceptional point, $\Delta\mathrm{Re}\,\gamma = \pm\pi/2$.

The case of $t = 2/\delta$ requires more careful analysis. Assuming $t = 2/\delta$ and inserting $\rho = \delta$ into equation (110), we obtain

$$\gamma = \pm\frac{\pi}{4} - \frac{4\omega}{3\delta} + \frac{\Delta - \omega}{\delta} - \frac{\mathrm{i}}{2}\ln\frac{\mathrm{e}^2|\Delta - \omega|}{2\delta + \mathrm{i}(\Delta - \omega)} + \mathcal{O}(\Omega^4), \tag{112}$$

where the upper/lower sign corresponds to $\rho - \delta \to \pm 0$. At the exceptional point we have (figure 8, left panel),

$$\mathrm{Re}\,\gamma = \pm\frac{\pi}{4} - \frac{4\omega}{3\delta}. \tag{113}$$

Similarly, assuming $\Delta - \omega = 0$, we obtain

$$\gamma = \pm\frac{\pi}{2} - \frac{4\omega\rho^2}{3\delta^3} - \frac{\mathrm{i}}{2}\ln\frac{|\rho^2 - \delta^2|\mathrm{e}^2}{\rho^2 + 5\delta^2} + \mathcal{O}(\Omega^4), \tag{114}$$

where the upper/lower sign corresponds to $\Delta - \omega \to \pm 0$. At the exceptional point, (figure 8, right panel),

$$\mathrm{Re}\,\gamma = \pm\frac{\pi}{2} - \frac{4\omega}{3\delta}. \tag{115}$$

4.1.3. Quantum evolution in the vicinity of degeneracy. To study the tunneling process near a degeneracy, we assume that $|u(t)\rangle$ is a solution of equation (89) with the initial state at $t = 0$ chosen to be $|u_\uparrow\rangle$, and the final state of the system at a later time t to be $|u_\uparrow\rangle$ or $|u_\downarrow\rangle$. Then following [20], we compute the probability $P_{\uparrow\uparrow}(P_{\downarrow\uparrow})$ that the system is in the state $|u_\uparrow\rangle$ ($|u_\downarrow\rangle$), respectively, as

$$P_{\uparrow\uparrow} = |\cos(\Omega t/2) - \mathrm{i}\cos\chi\,\sin(\Omega t/2)|^2\,\mathrm{e}^{-\lambda t} \tag{116}$$

$$P_{\downarrow\uparrow} = |\sin\chi\,\sin(\Omega t/2)|^2\,\mathrm{e}^{-\lambda t}. \tag{117}$$

In what follows, we restrict ourselves to the case $\omega = \Delta$. Then, according to the classification of table 1, a fictitious hyperbolic monopole emerges in the parameter space $\mathbb{R}^3$ defined by the parameters of the system $\mathrm{Re}\,V_0$, $\mathrm{Im}\,V_0$, $\delta \in \mathbb{R}^3$.

There are two different regimes dependent on the relation between ρ and δ. For $\rho > \delta$ we have *one-sheeted hyperbolic monopole* and *coherent* tunneling process

$$P_{\uparrow\uparrow} = \mathrm{e}^{-\lambda t}\left(\cos\frac{\Omega_0 t}{2} - \frac{\delta}{\Omega_0}\sin\frac{\Omega_0 t}{2}\right)^2, \tag{118}$$

$$P_{\downarrow\uparrow} = \mathrm{e}^{-\lambda t}\frac{\rho^2}{\Omega_0^2}\sin^2\frac{\Omega_0 t}{2}, \tag{119}$$

where $\Omega_0 = |\rho^2 - \delta^2|^{1/2}$ denotes the Rabi frequency.

On the other hand, for $\rho < \delta$, there is *incoherent* tunneling

$$P_{\uparrow\uparrow} = \mathrm{e}^{-\lambda t}\left(\cosh\frac{\Omega_0 t}{2} - \frac{\delta}{\Omega_0}\sinh\frac{\Omega_0 t}{2}\right)^2, \tag{120}$$

$$P_{\downarrow\uparrow} = \mathrm{e}^{-\lambda t}\frac{\rho^2}{\Omega_0^2}\sinh^2\frac{\Omega_0 t}{2} \tag{121}$$

and the associated monopole is the *two-sheeted hyperbolic monopole*. At the exceptional point, $\Omega_0 = 0$, and both regimes yield

$$P_{\uparrow\uparrow} = \left(1 - \frac{\delta t}{2}\right)^2\mathrm{e}^{-\lambda t} \qquad \text{and} \qquad P_{\downarrow\uparrow} = \left(\frac{\delta t}{2}\right)^2\mathrm{e}^{-\lambda t}. \tag{122}$$

The Rabi oscillations are manifested in the quantum oscillation between the up and down states and can be characterized by the following function: $P(t) = P_{\uparrow\uparrow} - P_{\downarrow\uparrow}$ [54]. The computation yields

$$P(t) = \mathrm{e}^{-\lambda t}\left(\cos(\Omega_0 t) - \frac{\delta}{\Omega_0}\sin(\Omega_0 t)\right), \qquad \text{if} \quad \rho > \delta \tag{123}$$

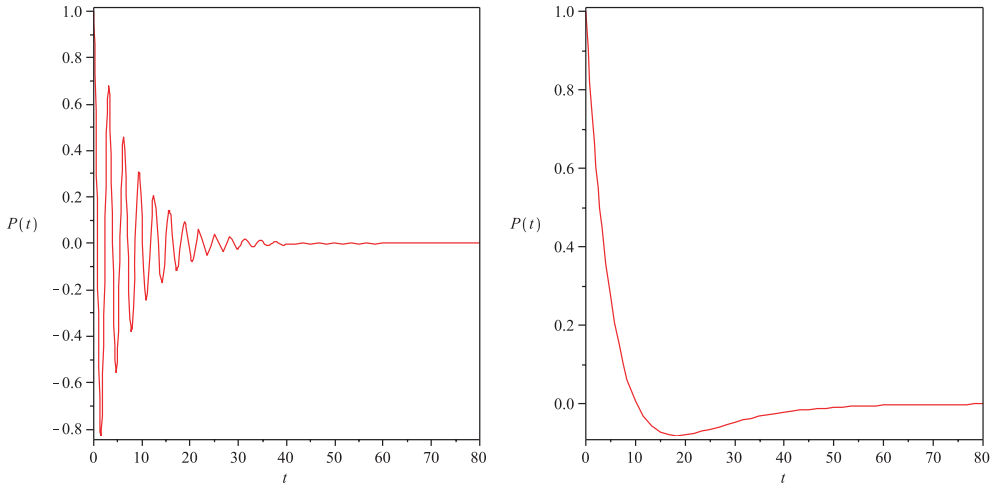

Figure 9. Left panel: the Rabi oscillation $P(t)$ as a function of t for coherent tunneling ($\rho > \delta, \Omega_0 = 0.025, \delta = 0.1, \lambda = 0.125$). It is manifested as the quantum oscillation between the up and down states, $|u_\uparrow\rangle$ and $|u_\downarrow\rangle$. Right panel: $P(t)$ versus t for incoherent tunneling ($\rho < \delta, \Omega_0 = 2, \delta = 0.1, \lambda = 0.125$).

$$P(t) = \mathrm{e}^{-\lambda t}\left(\cosh(\Omega_0 t) - \frac{\delta}{\Omega_0}\sinh(\Omega_0 t)\right), \qquad \text{if} \quad \rho < \delta \tag{124}$$

and at the exceptional point

$$P(t) = \mathrm{e}^{-\lambda t}\left(1 - \frac{\delta t}{2}\right). \tag{125}$$

The Rabi oscillation function $P(t)$ is plotted in figure 9. In addition, it is simple to show that in the absence of dissipation $P(t) = \cos(\Omega_0 t)$.

Returning our attention to the geometric phase defined by equation (109), we obtain

$$\gamma = \frac{\omega\left(\delta^2 + \Omega_0^2\right)}{2\Omega_0^3}(\sin\Omega_0 t - \Omega_0 t) - \mathrm{i}\frac{\delta t}{2} + \frac{\mathrm{i}}{2}\ln\frac{\Omega_0 + \delta\tan\frac{\Omega_0 t}{2}}{\Omega_0 - \delta\tan\frac{\Omega_0 t}{2}}, \qquad \text{if} \quad \rho > \delta \tag{126}$$

and

$$\gamma = \frac{\omega\left(\delta^2 + \Omega_0^2\right)}{2\Omega_0^3}(\sinh\Omega_0 t - \Omega_0 t) - \mathrm{i}\frac{\delta t}{2} + \frac{\mathrm{i}}{2}\ln\frac{\Omega_0 + \delta\tanh\frac{\Omega_0 t}{2}}{\Omega_0 - \delta\tanh\frac{\Omega_0 t}{2}}, \qquad \text{if} \quad \rho < \delta. \tag{127}$$

It follows from equation (126) that the real part of the geometric phase $\mathrm{Re}\,\gamma(t)$ has the jump discontinuity $\Delta\,\mathrm{Re}\,\gamma = \mp\pi/2$ at the points

$$t_n = \frac{2}{\Omega_0}\left(\pi n \pm \arctan\frac{\Omega_0}{\delta}\right), \qquad n = 0, 1, \ldots \tag{128}$$

with the pulse duration given by

$$\Delta t = \frac{2\pi}{\Omega_0}\left(1 - \frac{2}{\pi}\arctan\frac{\Omega_0}{\delta}\right). \tag{129}$$

For the incoherent tunneling defined by equation (127), the jump discontinuity $\Delta\,\mathrm{Re}\,\gamma = -\pi/2$ occurs at the point

$$t_0 = \frac{2}{\Omega_0}\tanh^{-1}\left(\frac{\Omega_0}{\delta}\right). \tag{130}$$

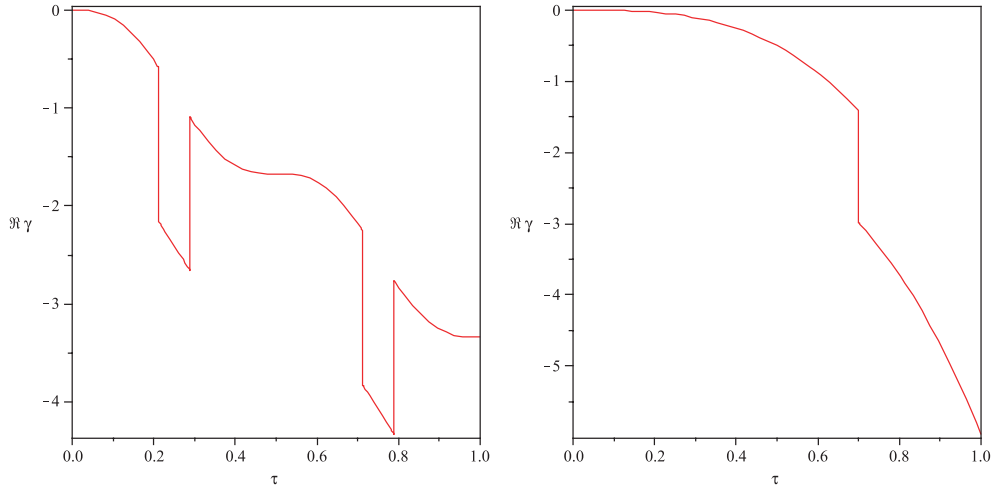

Figure 10. The real part of the geometric phase $\mathrm{Re}\,\gamma(\tau)$ versus time $\tau = 2\pi t/\omega$. Left panel (one-sheeted hyperbolic monopole): coherent tunneling ($\Omega_0 = 2, \delta = 0.5, \omega = 1$). Right panel (two-sheeted hyperbolic monopole): incoherent tunneling ($\Omega_0 = 0.25, \delta = 0.5, \omega = 1$).

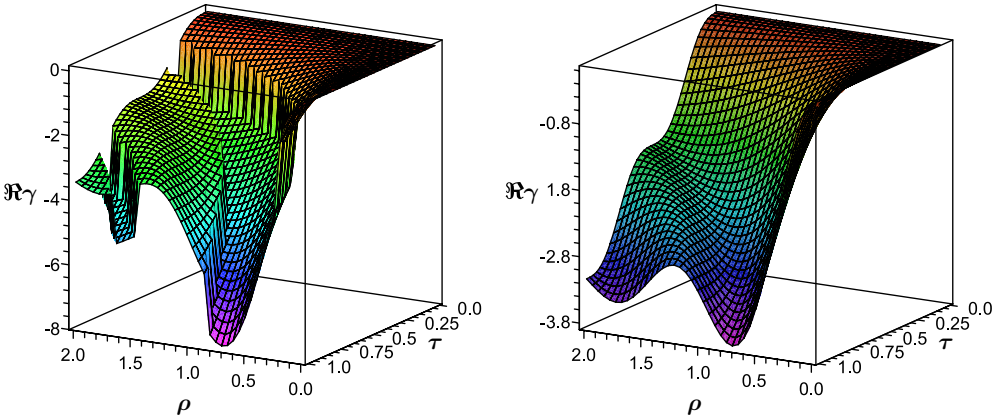

Figure 11. Hyperbolic monopole. The real part of the geometric phase $\mathrm{Re}\,\gamma(\tau)$ versus time $\tau = 2\pi t/\omega$ and ρ is depicted. Left panel: dissipative system $\delta \neq 0$ ($\delta = 0.5, \omega = 1$). Right panel: $\mathrm{Re}\,\gamma(\tau)$ is plotted in the absence of dissipation ($\delta = 0, \omega = 1$). As can be seen from the plot, the pulses presented at the left have disappeared.

At the exceptional point, $\Omega_0 = 0$, we have $t_0 = 2/\delta$ and the pulse duration $\Delta t \to \infty$. In the absence of dissipation ($\delta = 0$) the pulses disappear. Indeed, in the limit $t_0 = 2/\delta \to \infty$, and in addition, the pulse duration $\Delta t \to 0$ while $\delta t \to 0$. The real part of the non-adiabatic geometric phase, $\mathrm{Re}\,\gamma(\tau)$, as a function of the time $\tau = 2\pi t/\omega$ is plotted in figure 10, and in figure 11 the real part of the geometric phase $\mathrm{Re}\,\gamma(\tau, \rho)$ versus τ and ρ is depicted.

To conclude, we note that the transition at the exceptional $\rho = \delta$ between two tunneling regimes is the topological phase transition in parameter space, which can be described by a two-sheeted hyperbolic monopole ($\rho < \delta$) $\leftrightarrow$ one-sheeted hyperbolic monopole ($\rho > \delta$).

5. Conclusion

In this paper, we considered the geometric phase and quantum tunneling in the vicinity of diabolic and exceptional points. We demonstrated that the complex geometric phase associated with the degeneracy points is defined by the flux of the complex fictitious 'magnetic' monopole. In the weak-coupling limit, the leading contribution to the real part of the geometric phase is given by the flux of the Dirac monopole plus a quadrupole term, and the expansion of the imaginary part starts with a dipole-like field. Recently, a similar result was obtained for a two-level spin-half system in a slowly varying magnetic field, weakly coupled to a dissipative environment [55].

We found that the real part of the complex geometric phase has a discontinuity at the exceptional point. We have also shown that the exceptional point is the critical point of the quantum mechanical system, and a topological phase transition occurs at the exceptional point.

We identified two different regimes when studying the tunneling process near and at the exceptional point: coherent and incoherent. Coherent tunneling is characterized by Rabi oscillations, also known as quantum echoes, and it has been shown that the dissipation results in pulses in the real part of the geometric phase. At the exceptional point, both tunneling regimes exhibit a quadratic dependence in time that is in accordance with the results obtained in [56, 57] for some specific non-Hermitian systems. The decay behavior predicted by equations (118)–(122) has recently been observed in experiments with a dissipative microwave billiard [57].

The emergence of pulses in the geometric phase is a novel quantum phenomenon, which reflects the monopole structure of the system. This complex-valued phase effect may be detected using quantal dissipative interferometry [58, 59]. Note that such strong coupling with the environment should take place in generic dissipative systems, since in the neighborhood of the exceptional point only terms related to the invariant subspace formed by the two-dimensional Jordan block make substantial contributions, which makes the N-dimensional problem become effectively two-dimensional [39, 41]. We conclude by remarking that the obtained results could be important in the implementation of fault-tolerant quantum computation, but it would be necessary to better understand the relation between geometric phase and decoherence to perform this computation [60, 61].

Acknowledgments

We thank A B Klimov, J L Romero, S G Ovchinnikov, U Günther, M S Plyushchay, I Rotter and B F Samsonov for helpful discussions and comments. This work is supported by research grants SEP-PROMEP 103.5/04/1911 and CONACyT U45704-F.

Appendix. Geometric phase for general evolution on the complex Bloch sphere

In this appendix, we derive from the general definition of the geometric phase (27) written for two-level system as

$$\gamma(\tau) = \frac{\mathrm{i}}{2}\ln\left(\frac{\langle\tilde{u}(\tau)|u(0)\rangle}{\langle\tilde{u}(0)|u(t)\rangle}\right) + \mathrm{i}\int_0^\tau \langle\tilde{u}(t)|\frac{\mathrm{d}}{\mathrm{d}t}|u(t)\rangle\,\mathrm{d}t \tag{A.1}$$

formula (71) for the computation of the geometric phase in terms of the complex Bloch vector. Equation (A.3) generalizes to a non-Hermitian Hamiltonian the formula obtained by Zang and Wang for the computation of the nonadiabatic noncyclic geometric phase for the Hermitian two-level system [62].

Theorem. *The complex geometric phase defined in equation (A.1) is given on the complex Bloch sphere* S_c^2 *by*

$$\gamma(\tau) = -\frac{1}{2}\int_0^\tau \frac{n_1\dot{n}_2 - n_2\dot{n}_1}{1+n_3}\,\mathrm{d}t + \arctan\left(\frac{\sin(\beta_f-\beta_i)}{\cot(\alpha_f/2)\cot(\alpha_i/2)+\cos(\beta_f-\beta_i)}\right), \tag{A.2}$$

where integration is performed along the unique curve $\mathbf{n}(t)$ *on the unit sphere* S_c^2*, joining the initial point* $\mathbf{n}(0) = (\sin\alpha_i\cos\beta_i, \sin\alpha_i\sin\beta_i, \cos\alpha_i)$ *and the final point* $\mathbf{n}(\tau) = (\sin\alpha_f\cos\beta_f, \sin\alpha_f\sin\beta_f, \cos\alpha_f)$.

Proof. In the general form, for a two-level system in terms of column and row vectors we have

$$|u(t)\rangle = \begin{pmatrix} a(t) \\ b(t) \end{pmatrix}, \qquad \langle\tilde{u}(t)| = (\tilde{a}(t), \tilde{b}(t)). \tag{A.3}$$

After some algebra and using the definition of the Bloch vector $\mathbf{n}(t) = \langle\widetilde{\Psi}(t)|\boldsymbol{\sigma}|\Psi(t)\rangle$, we find

$$n_1(t) = a\tilde{b} + \tilde{a}b, \qquad n_2(t) = \mathrm{i}(a\tilde{b} - \tilde{a}b), \qquad n_3(t) = a\tilde{a} - b\tilde{b}. \tag{A.4}$$

From here, setting $\mathbf{n}(t) = (\sin\alpha\cos\beta, \sin\alpha\sin\beta, \cos\alpha)$, we obtain

$$a\tilde{b} = \sin\frac{\alpha}{2}\cos\frac{\alpha}{2}\,\mathrm{e}^{-\mathrm{i}\beta}, \qquad a\tilde{a} = \cos^2\frac{\alpha}{2}, \tag{A.5}$$

$$\tilde{a}b = \sin\frac{\alpha}{2}\cos\frac{\alpha}{2}\,\mathrm{e}^{\mathrm{i}\beta}, \qquad b\tilde{b} = \sin^2\frac{\alpha}{2}. \tag{A.6}$$

Next, denoting by $|u_i\rangle$ and $|u_f\rangle$ the initial and final states, respectively, we can write the total phase as follows:

$$\gamma_t = \frac{\mathrm{i}}{2}\ln\left(\frac{\langle\tilde{u}(\tau)|u(0)\rangle}{\langle\tilde{u}(0)|u(t)\rangle}\right) = \frac{\mathrm{i}}{2}\ln\left(\frac{\langle\tilde{u}_f|u_i\rangle}{\langle\tilde{u}_i|u_f\rangle}\right) = \frac{\mathrm{i}}{2}\ln\left(\frac{\tilde{a}_f a_i + \tilde{b}_f b_i}{\tilde{a}_i a_f + \tilde{b}_i b_f}\right). \tag{A.7}$$

Then, applying (A.5) and (A.6), we obtain

$$\gamma_t = \frac{\mathrm{i}}{2}\ln\left(\frac{\cot(\alpha_f/2)\cot(\alpha_i/2) + \mathrm{e}^{\mathrm{i}(\beta_i-\beta_f)}}{\cot(\alpha_f/2)\cot(\alpha_i/2) + \mathrm{e}^{\mathrm{i}(\beta_f-\beta_i)}}\right) + \frac{\mathrm{i}}{2}\ln\left(\frac{a_i\tilde{a}_f}{a_f\tilde{a}_i}\right). \tag{A.8}$$

This yields

$$\gamma_t = \arctan\left(\frac{\sin(\beta_f-\beta_i)}{\cot(\alpha_f/2)\cot(\alpha_i/2)+\cos(\beta_f-\beta_i)}\right) + \frac{\mathrm{i}}{2}\int_0^\tau\left(\frac{\mathrm{d}\tilde{a}}{\tilde{a}} - \frac{\mathrm{d}a}{a}\right). \tag{A.9}$$

Since the dynamical phase

$$\gamma_d = -\mathrm{i}\int_0^\tau \langle\tilde{u}(t)|\frac{\mathrm{d}}{\mathrm{d}t}|u(t)\rangle\,\mathrm{d}t = -\mathrm{i}\int_0^\tau(\tilde{a}\dot{a} + \tilde{b}\dot{b})\,\mathrm{d}t, \tag{A.10}$$

we obtain

$$\gamma = \gamma_t - \gamma_d = \arctan\left(\frac{\sin(\beta_f-\beta_i)}{\cot(\alpha_f/2)\cot(\alpha_i/2)+\cos(\beta_f-\beta_i)}\right) + \mathrm{i}\int_0^\tau\left((\tilde{a}\dot{a} + \tilde{b}\dot{b}) + \frac{1}{2}\left(\frac{\dot{\tilde{a}}}{\tilde{a}} - \frac{\dot{a}}{a}\right)\right)\mathrm{d}t. \tag{A.11}$$

Using the relations (A.4)–(A.6), we find

$$(1-\cos\alpha)\dot{\beta} = \frac{n_1\dot{n}_2 - n_2\dot{n}_1}{1+n_3} = -2\mathrm{i}\left((\tilde{a}\dot{a} + \tilde{b}\dot{b}) + \frac{1}{2}\left(\frac{\dot{\tilde{a}}}{\tilde{a}} - \frac{\dot{a}}{a}\right)\right). \tag{A.12}$$

Then, inserting this result into (A.11), we obtain

$$\gamma(\tau) = -\frac{1}{2}\int_0^\tau \frac{n_1\dot{n}_2 - n_2\dot{n}_1}{1+n_3}\,\mathrm{d}t + \arctan\left(\frac{\sin(\beta_f-\beta_i)}{\cot(\alpha_f/2)\cot(\alpha_i/2)+\cos(\beta_f-\beta_i)}\right). \tag{A.13}$$

□

Corollary. *The geometric phase can be calculated by the following integral*

$$\gamma(\tau) = -\frac{1}{2}\int_0^\tau (1-\cos\alpha)\dot{\beta}\mathrm{d}t + \arctan\left(\frac{\sin(\beta_f-\beta_i)}{\cot(\alpha_f/2)\cot(\alpha_i/2)+\cos(\beta_f-\beta_i)}\right). \tag{A.14}$$

References

[1] Fang Z *et al* 2003 Anomalous Hall effect and magnetic monopoles in momentum-space *Science* **302** 92–5
[2] Zhang P, Li Y and Sun C P 2005 Induced magnetic monopole from trapped Λ-type atom *Eur. Phys. J.* D **36** 229–33
[3] Bhandari R 2002 Singularities of the mixed state phase *Phys. Rev. Lett.* **89** 268901
[4] Haldane F D M 2004 Berry curvature on the Fermi surface anomalous Hall effect as a topological Fermi-liquid property *Phys. Rev. Lett.* **93** 206602
[5] Frenkel J and Pereira S H 2004 Coordinate noncommutativity in strong non-uniform magnetic fields *Phys. Rev.* D **69** 127702
[6] Savage C M and Ruostekoski J 2003 Dirac monopoles and dipoles in ferromagnetic spinor Bose–Einstein condensates *Phys. Rev.* A **68** 043604
[7] Murakami S and Nagaosa N 2003 Berry phase in magnetic superconductors *Phys. Rev. Lett.* **90** 057002
[8] Barouch Eytan and McCoy Barry M 1971 Statistical mechanics of the *XY* model. II: spin-correlation functions *Phys. Rev.* A **3** 786–804
[9] Berry M V 1984 Quantal phase factor accompanyng adiabatic changes *Proc. R. Soc.* A **392** 45–57
[10] Berry M V and Wilkinson M 1984 Diabolical points in the spectra of triangles *Proc. R. Soc.* A **392** 15–43
[11] Berry M V and Dennis M R 2003 The optical singularities of birefringent dichroic chiral crystals *Proc. R. Soc.* A **459** 1261–92
[12] Simon B 1983 Holonomy the quantum adiabatic theorem, and Berry's phase *Phys. Rev. Lett.* **51** 2167–70
[13] Garrison J C and Wright E M 1988 Complex geometrical phases for dissipative systems *Phys. Lett.* A **128** 177–81
[14] Nesterov A I and Aceves de la Cruz F 2006 Complex magnetic monopoles and geometric phases around diabolic and exceptional points arXiv:quant-ph/0611280
[15] Berry M V 2004 Physics of nonhermitian degeneracies *Czech. J. Phys.* **54** 1039–47
[16] Heiss W D 2004 Exceptional points of non-Hermitian operators *J. Phys. A: Math. Gen.* **37** 2455–64
[17] Heiss W D 2004 Exceptional points their universal occurrence and their physical significance *Czech. J. Phys.* **54** 1091–99
[18] Carollo A, Fuentes-Guridi I, França Santos M and Vedral V 2003 Geometric phase in open system *Phys. Rev. Lett.* **90** 160402
[19] Plenio M B and Knight P L 1998 The quantum-jump approach to dissipative dynamics in quantum optics *Rev. Mod. Phys.* **70** 101–44
[20] Baker H C 1984 Non-Hermitian quantum theory of multiphoton ionization *Phys. Rev.* A **30** 773–93
[21] Latinne O, Kylstra N J, Dörr M, Purvis J, Terao-Dunseath M, Joachain C J, Burke P G and Noble C J 1995 Laser-induced degeneracies involving autoionizing states in complex atoms *Phys. Rev. Lett.* **74** 46–9
[22] Philipp M, Brentano P von, Pascovici G and Richter A 2000 Frequency and width crossing of two interacting resonances in a microwave cavity *Phys. Rev.* E **62** 1922–26
[23] Oberthaler M K, Abfalterer R, Bernet S, Schmiedmayer J and Zeilinger A 1996 Atom waves in crystals of light *Phys. Rev. Lett.* **77** 4980–3
[24] Dembowski C, Graf H-D, Harney H L, Heine A, Heiss W D, Rehfeld H and Richter A 2001 Experimental observation of the topological structure of exceptional points *Phys. Rev. Lett.* **86** 787–90
[25] Stehmann T, Heiss W D and Scholtz F G 2004 Observation of exceptional points in electronic circuits *J. Phys. A: Math. Gen.* **37** 7813–9
[26] Berry M V 1990 *Quantum adiabatic anholonomy Anomalies, Phases, Defects (Naples) (Bibliopolis)* ed U M Bregola, G Marino and G Morandi p 125
[27] Berry M V 1995 Two-state quantum asymptotic *Ann. NY Acad. Sci.* **755** 303–17
[28] Berry M V 2006 Proximity of degeneracies and chiral points *J. Phys. A: Math. Gen.* **39** 10013–8

[29] Gao X-C, Xu J-B and Qian T-Z 1992 Invariants and geometric phase for systems with non-Hermitian time-dependent Hamiltonians *Phys. Rev.* A **46** 3626–30
[30] Heiss W D 2003 Global and local aspects of exceptional points arXiv:quant-ph/0211090
[31] Heiss W D and Harney H L 2001 The chirality of exceptional points *Eur. Phys. J.* D **17** 149–51
[32] Keck F, Korsh H J and Mossman S 2003 Unfolding a diabolic point a generalized crossing scenario *J. Phys. A: Math. Gen.* **36** 2125–37
[33] Keck F and Mossman S 2003 Stark resonances for a double δ quantum well crossing scenarios, exceptional points and geometric phases *J. Phys. A: Math. Gen.* **36** 2139–53
[34] Dattoli G, Mignani R and Torre A 1990 Geometrical phase in the cyclic evolution of non-Hermitian systems *J. Phys. A: Math. Gen.* **23** 5795–806
[35] Aharonov Y, Massar S, Popescu S, Tollaksen J and Vaidman L 1996 Adiabatic measurements on metastable systems *Phys. Rev. Lett.* **77** 983–7
[36] Massar S 1996 Applications of the complex geometric phase for metastable systems *Phys. Rev.* A **54** 4770–74
[37] Mondragón A and Hernández E 1996 Berry phase of resonant states *J. Phys. A: Math. Gen.* **29** 2567–8
[38] Moiseyev N and Narevicius E 2006 Non-Hermitian quantum mechanics formalism and applications *Fundamental World of Quantum Chemistry: A Tribute to the Memory of Per-Olov Löwdinon* vol 2 ed E J Brndas and Eugene S Kryachko (Berlin: Springer) pp 1–32
[39] Arnold V I 1983 *Geometric Methods in the Theory of Ordinary Differential Equations* (New York: Springer)
[40] Morse P M and Feshbach H 1953 *Methods of Theoretical Physics* (New York: McGraw-Hill)
[41] Kirillov O N, Mailybaev A A and Seyranian A P 2005 Unfolding of eigenvalue surfaces near a diabolic point due to a complex perturbation *J. Phys. A: Math. Gen.* **38** 5531–46
[42] Seyranian A P, Kirillov O N and Mailybaev A A 2005 Coupling of eigenvalues of complex matrices at diabolic and exceptional points *J. Phys. A: Math. Gen.* **38** 1723–40
[43] Mailybaev A A, Kirillov O N and Seyranian A P 2005 Geometric phase around exceptional points *Phys. Rev.* A **72** 014104
[44] Günther U, Rotter I and Samsonov B F 2007 Projective Hilbert space structures at exceptional points *J. Phys. A: Math. Theor.* **40** 8815–33
[45] Aharonov Y and Anandan J 1987 Phase change during a cyclic quantum evolution *Phys. Rev. Lett.* **58** 1593–6
[46] Anandan J and Stodolsky L 1987 Some geometrical considerations of Berry's phase*Phys. Rev.* D **35** 2597–600
[47] Lévay P and Apagyi B 1993 Algebraic scattering theory and the geometric phase *Phys. Rev.* A **47** 823–30
[48] Jackiw R 1989 *Three Elaboration on Berry's Connection, Curvature and phase Advanced Series in Mathematical Physics* vol 5 (Singapore: World Scientific) pp 29–41 chapter 1
[49] Vinet L 1988 Invariant Berry connections *Phys. Rev.* D **37** 2369–72
[50] Schonfeld J F 1981 A mass term for three-dimensional gauge fields *Nucl. Phys.* B **185** 157–71
[51] Plyushchay M S 2006 Majorana equation and exotics higher derivative models, anyons and noncommutative geometry *Electron. J. Theor. Phys.* **3** 17–31
[52] Chu Shih-I, Zhong-Chao Wu and Layton Eric 1989 Density matrix formulation of complex geometric quantum phases in dissipative systems *Chem. Phys. Lett.* **157** 151–8
[53] Lamb W E, Schlicher R R and Scully M O 1987 Matter–field interaction in atomic physics and quantum optics *Phys. Rev.* A **36** 2763–2772
[54] Wu C-Q, Li J-X and Lee D-H 2007 Phase transition in a two-level-cavity system in an ohmic environment arXiv:cond-mat/0703238
[55] Whitney R S, Makhlin Y, Shnirman A and Gefen Y 2005 Geometric nature of the environment-induced Berry phase and geometric dephasing *Phys. Rev. Lett.* **94** 070407
[56] Stafford C A and Barrett B R 1999 Simple model for decay of superdeformed nuclei *Phys. Rev.* C **60** 051305
[57] Dietz B, Friedrich T, Metz J, Miski-Oglu M, Richter A, Schafer F and Stafford C A 2007 Rabi oscillations at exceptional points in microwave billiards *Phys. Rev.* E **75** 027201
[58] Sjöqvist E, Pati A K, Ekert A, Anandan J S, Ericsson M, Oi D K L and Vedral V 2000 Geometric phases for mixed states in interferometry *Phys. Rev. Lett.* **85** 2845–9
[59] Sjöqvist E 2004 Quantal interferometry with dissipative internal motion *Phys. Rev.* A **70** 052109
[60] Jones J A, Vedral V, Ekert A and Castagnoli G 2000 Geometric quantum computation using nuclear magnetic resonance *Nature* **403** 869–71
[61] Zhu Shi-Liang and Wang Z D 2003 Unconventional geometric quantum computation *Phys. Rev. Lett.* **91** 187902
[62] Zhu Shi-Liang, Wang Z D and Zhang Yong-Dong 2000 Nonadiabatic noncyclic geometric phase of a spin-$\frac{1}{2}$ particle subject to an arbitrary magnetic field *Phys. Rev.* B **61** 1142–48